

Regular article

Electronic excitation of sulfur-organic compounds – performance of time-dependent density functional theory

Jürgen Fabian

Institut für Organische Chemie, Technische Universität Dresden, Mommsenstrasse 13, 01062 Dresden, Germany

Received: 30 October 2000 / Accepted: 29 November 2000 / Published online: 22 May 2001

© Springer-Verlag 2001

Abstract. To define the scope and limitations of the time-dependent density functional theory (TDDFT) method, spectral absorption data of a series of about 100 neutral or charged sulfur-organic compounds with up to 24 non-hydrogen atoms and up to four sulfur atoms were calculated in the near-UV, visible and IR regions. Although the theoretical vertical transition energies correspond only approximately to experimental absorption band maxima, the mean absolute deviation was calculated to be 0.21 eV (1600 cm^{-1}). The main absorption features of various compounds with mono-coordinated or dicoordinated sulfur atoms are well reproduced. As far as possible TDDFT results were compared with those of semiempirical Zerner's intermediate neglect of differential overlap (ZINDO/S) and of Pariser–Parr–Pople (PPP) calculations. TDDFT also works well in cases where the semiempirical methods fail. Limitations of TDDFT were encountered with calculations of spectral absorptions of dye molecules. The “vinylene shift” of polymethine dyes is not reproduced by TDDFT. Whereas electronic excitation energies delocalized polar and betainic chromophores are reasonably well reproduced, excitation energies of charge-transfer-type and charge-resonance-type transitions of weakly interacting composite chromophores are significantly underestimated.

Key words: Sulfur-organic compounds – Dyes – Time-dependent density functional theory – Zerner's intermediate neglect of differential overlap – Pariser–Parr–Pople

1 Introduction

If light absorption occurs in the experimentally easily accessible spectral region longer than 200 nm the characteristics of the electronic spectra may play a considerable role in structural analysis. Compounds absorbing light between about 400 and 800 nm are

colored. Conjugated organic compounds generally exhibit spectral absorptions in the near UV (NUV), visible and sometimes in the near-IR region (NIR). The absorption wavelengths depend on the molecular and electronic structure. Because of the delocalized nature of the electronic excitation, empirical spectroscopic increments are of little value in UV/vis/NIR spectroscopy. Quantum chemical methods have rather to be used to predict and rationalize spectral absorption data. For planar conjugated compounds the semiempirical Pariser–Parr–Pople (PPP) method [1] developed in the mid-1950s is very useful. This method enables spectral absorptions caused by $\pi\rightarrow\pi^*$ transitions to be calculated. The PPP calculation makes use of a limited configuration interaction (CI) of singly excited configurations. The extension of the PPP approximation to the all-valence electron system [2] was based on the complete neglect of differential overlap (CNDO) or intermediate neglect of differential overlap (INDO) methodologies developed by Pople and coworkers. Application to spectroscopy required a modification of the methods. The resulting methods were CNDO/S, INDO/S, LNDO/S (local neglect of differential overlap), CNDOL (azimuthal quantum number 1 dependency) and other related methods. These methods were parameterized for sulfur-containing compounds [2, 3]. To better match the maximum absorption wavelengths Ridley and Zerner [4] introduced a weighting of both the π -type and σ -type overlap. This method, known as Zerner's intermediate neglect of differential overlap (ZINDO/S), is readily available from commercial program packages. Like PPP this method was primarily parameterized with spectral data of planar cyclic conjugated compounds. It is also a single configuration CI method. The method was mainly tested and applied for calculations of $\pi\rightarrow\pi^*$ and $n\rightarrow\pi^*$ transitions of compounds with first-row elements of the periodic chart [4]. ZINDO/S also allows the calculation of sulfur-organic compounds [5]. Neglect of diatomic differential overlap CI methods such as MNDO-CI (modified neglect of differential overlap), AM1-CI (Austin model 1) and PM3-CI (parametrized model 3) are used without scaling [6], whereas MNDO/C takes

into account the correlation effect with modified MNDO parameter sets [7].

The simplest ab initio approach to calculate transition energies is the Hartree–Fock-based singles-only CI method (CIS) and the random-phase approximation (RPA) [8]. Excitation energies calculated by these methods are much too low. The equation-of-motion method with coupled-cluster reference states (EOM–CCSDT) [9], the multireference configuration interaction method (MRCI) [10] and the multiconfigurational self-consistent-field method including second-order perturbation theory (CASSCF/CASPT2) [11] are high-level ab initio methods with a good performance in calculating transition energies. EOM–CCSD(T) is a response theory approach directed at the calculation of energy differences. The ground-state calculation is followed by the solution of a resonance eigenvalue equation that gives the vertical excitation energy directly. The spectrum is predicted in a single essentially black box calculation. On the other hand, multiconfigurational methods calculate the two states involved in the electron transition explicitly and independently. Since the active space in a CASSCF calculation has to be chosen for each state, the calculation becomes exceedingly difficult for larger compounds. In spite of the difficult choice of the active space and other user-determined computational choices in CASSCF/CASPT2 calculations, Roos and coworkers calculated a representative series of organic compounds [11] including three sulfur-containing compounds, thiophene, bithiophene and terthiophene [12]. Multiconfigurational methods require extended basis sets. The calculations are computationally demanding for larger compounds and are expensive with atoms of second- or higher-row elements. Because of the high expenditure these methods are less attractive in deriving relationships between spectral absorption (color) and structure.

On the other hand, the more recently developed electron-density-based methods find increasing interest in calculations of electron transition energies [13–22]. According to the first results time-dependent density functional theory (TDDFT) is a good compromise between accuracy and computational efficiency. Like EOM–CCSD(T), TDDFT is a response method. The whole spectrum is calculated in a single run. The computational costs are much lower than those of the high-level ab initio calculations. Extended basis sets are not required. When the one-electron basis set and the functional are chosen the complete set of excitation energies is available. A disadvantage of the method is the fact that performance can hardly be improved without introduction of better functionals, which are, however, not available in any straightforward way. In addition, two-electron excitations are not calculated and the Rydberg-type transition energy may be seriously in error. Fortunately these transitions generally occur only at higher energies. Modified TDDFT methods were put forward, such as TDDFT in the Tamm–Dancoff approximation [23] and DFT/CIS [24, 25] and DFT/MRCI methods [26], including, in part, few empirical parameters. The more approximate and, therefore, more efficient density functional–tight binding (DFTB)–time-dependent local density approximation (TDLDA)

method recently developed [27] makes use of the local density approximation. The deviations between TDDFT-calculated and experimental excitation energies were reported to be between 0.0 and 1.0 eV [14, 18, 19, 22]. The average accuracy for polycyclic hydrocarbons is about 0.3 eV [19]. A first systematic comparison of results of TDDFT calculations and CASPT2 calculations has been made recently [22]. In the last mentioned study attention was mainly placed on compounds that absorb in the short wavelengths region of the UV, where both valence-type and Rydberg-type transitions are important. The comparison revealed that the two methods give similar results, in general, but TDDFT may exhibit erratic behavior in the high-energy region. Although encouraging results were reported with the study of the pigments porphyrin [14, 16, 21] and chlorophyll [20], the performance of TDDFT is less well known for compounds with absorptions at longer wavelengths. Except for the thiophene parent compound [22] sulfur-organic chromophores were apparently not calculated by TDDFT. We recently reported calculations of spectral data of thiocumulenes that were found to be about 0.2 eV in error with respect to the few experimental data available [28]. In addition, the enigma of the color of 1,2-dithiin [29] was solved: while semiempirical all-valence electron calculations and ab initio CIS calculations failed in predicting the long-wavelength absorption, TDDFT calculations resulted in the experimentally found color band. The nature of the color band was discussed in terms of the Kohn–Sham orbitals involved in the electronic transition.

The aim of this work is to evaluate the performance of the TDDFT method by examining a series of about 100 sulfur-organic compounds of quite different structure. Compounds with monocoordinated (C=S) and dicoordinated sulfur (-S-) are mainly considered, with various planar or nonplanar structures. Owing to the presence of sulfur atoms these compounds absorb, in general, at relatively long wavelengths. The spectra cover the NUV and possibly the visible and NIR region.

2 Computational details

The TDDFT program used is part of the GAUSSIAN98 suite of programs [30]. Becke's three-parameter Lee–Yang–Parr functional (B3-LYP) [31] has been widely used in the calculation of molecular geometries and parameters of organic compounds. The functional has also been tested in TDDFT calculations [14, 16, 17, 21, 22]. Since the results of the calculations are hardly dependent on the basis set the early recommended [16] 6-31+G* basis set was used throughout this work. The B3-LYP/6-31+G* approximation was also employed in optimizing the molecular geometries in this study except for some larger molecules where the lower level B3-LYP/3-21G geometries were taken (**24**, **55**, **59** and **60**). Along these lines, geometry optimization and TDDFT calculations were done in a single run through a checkpoint file. The effect of diffuse functions is less marked on the geometrical parameters than on the spectral data. The comparison between the calculated DFT B3-LYP bond lengths and the experimental gas-phase structural data of thioacrolein (**3**), dimethyl sulfide (**13**), methylvinylsulfide (**17**), dimethyl disulfide (**21**), 1,2-dithiin (**23**), thiophene (**26**) and 4*H*-thiopyranthione (**25**) (r_{g} - or r_{s} - geometries [32]) showed an absolute mean deviation of 0.010 Å for CC (nine values), 0.019 Å for CS (nine values) and 0.06 Å for SS (two values). As is well known, bond

lengths of higher-period elements are overestimated by DFT B3-LYP calculations [33]. In spite of the lower accuracy of the latter geometries the spectral data calculated by B3-LYP/6-31+G* and by experimental geometries differ by few nanometers only (cf. [28, 29]). For the sake of comparison, B3-LYP optimized geometries were also used in the semiempirical calculations. ZINDO/S calculations were carried out using the program contained in GAUSSIAN98 using the default option (10×10 singly excited configurations) and PPP calculations using the program wPSIN3 [34] including up to 10×10 singly-excited $\pi\pi^*$ configurations in the CI. CC bond alternation was taken into account by the variable β technique [35]. The PPP parameters of monocoordinated and dicoordinated sulfur were given in previous articles [36–39].

The theoretical intensity was evaluated as the oscillator strength, f , calculated in the dipole length representation. As is well known, oscillator strengths are strongly dependent on the theoretical model. They are considerably overestimated in semiempirical approximations. For a correct calculation of TDDFT oscillator strengths release A7 of GAUSSIAN98 had to be used. Data for experimental oscillator strengths are scarce and may be less accurate when the absorption spectrum contains the overlap of several absorption bands. Nonetheless, calculated oscillator strengths are very helpful in assigning calculated electronic transitions to experimental absorption bands. As is well known, these values vary roughly linearly with the experimentally known molar absorption coefficients, ϵ , given in units of reciprocal molar centimeters, which is equivalent to centimeters squared per millimole, in this article. Thus, theoretical oscillator strengths are listed along with the calculated transition energies (absorption wavelengths) and the experimental log ϵ values. Unfortunately, knowledge of experimental polarization measurements for supporting spectral assignments is scarce.

3 Results and discussion

In selecting spectra, those with a well-separated band structure were preferred. In general, absorption data of larger sulfur-containing compounds are only available in solution. The absorption bands measured under these conditions have no vibrational fine structure in most cases. To avoid conformational isomers, most of the compounds selected were structurally rigid. The calculated transition energies are given in electron volts. Since chemists generally prefer spectral data in the unit of wavelengths, calculated and experimental values are compared in wavelengths. The wavelength is reciprocally related to energy and the error in the wavelength therefore increases with ascending wavelengths. The statistical evaluation of the performance of TDDFT, however, will refer to energy. Theoretical and experimental data of a representative series of sulfur-organic compounds are collected in Table 1 (compounds **1–50**).

The classification of the electronic transitions makes use of Kasha's short notation for one-electron transitions, i.e. $\sigma \rightarrow \pi^*$, $\pi \rightarrow \pi^*$, etc. [40]. In this study this classification scheme is also used if the compounds are not fully planar or if they are slightly perturbed by substituent groups. A slight departure from planarity does not much alter the nature of the orbitals and one-electron transitions. This classification scheme is not used, however, when the structures are more strongly puckered, although the orbitals may contain well-defined local contributions of n or π character. The orbitals were depicted using the program MOLDEN [41]. The symmetry of the molecules is indicated by the

point groups in Table 1 and the excited states by the irreducible representations as defined within the point group.

The theoretical values given in Table 1 are restricted to the wavelength region studied experimentally. Calculated spectral data obtained by semiempirical ZINDO/S and PPP calculations are listed in Table 1 for comparison. Results of the compounds **1–50** are discussed in the following two sections. Some more specific problems connected with the dye chromophores **51–75** are considered next.

3.1 Compounds with monocoordinated sulfur

Thiocarbonyl compounds are characterized by low-energy $n \rightarrow \pi^*$ transitions. The position of the first absorption band, and consequently of the color, varies strongly with the structure [42]. Whereas this type of absorption band is well understood, the nature of the two shorter-wavelength absorption bands of unsaturated thiocarbonyls is less clear and may be due to either the $\pi \rightarrow \pi^*$ or the $\sigma \rightarrow \pi^*$ transition. In analogy to carbonyl compounds Rosengren [43] tentatively assigned the two UV absorption bands of thiols to the $n \rightarrow \sigma^*$ and $\pi \rightarrow \pi^*$ transition. The assignment was later inverted when the spectral solvent effect of thiones was known [44]. In gas-phase spectra a Rydberg-type $n \rightarrow 4s$ transition was found in place of the $n \rightarrow \sigma^*$ type transition [45]. This assignment was backed by multireference doubly excited -CI calculations of Peyerimhoff et al. [46]. Measurement of adamantanethione in the gas phase as well as in solvent led to the conclusion that both transitions may be related [47]. At any rate, the transition in solution should have valence-type rather than Rydberg-type character [48]. The TDDFT calculation of thioformaldehyde without Rydberg-type functions led to an interpretation in terms of valence-type transitions.

Thioacetone (**1**) and thioamphor (**2**) are two saturated thioketones calculated in this study. As shown in Table 1 these compounds exhibit three transitions in the NUV/vis region. Within the TDDFT model the second transition is essentially of the $n \rightarrow \sigma^*$ type [28]. In agreement with experimental knowledge the $n \rightarrow \sigma^*$ transition of **1** occurs at lower energies than the $\pi \rightarrow \pi^*$ transition, while the opposite is true for **2**. Also reproduced by TDDFT, a strong redshift of the $n \rightarrow \pi^*$ absorption wavelength occurs in passing from the saturated compounds **1** and **2** to the unsaturated thiocarbonyl compounds **3–6**. Thiobenzaldehyde (**5**) was calculated to absorb at nearly the same wavelengths as thioacrolein (**3**). In the case of **3**, the n orbital is visualized in Fig. 1. As is to be expected by orbital overlap, the n orbital of thioacrolein is not strictly localized at sulfur. This holds for thiones more generally. In agreement with the experimental findings the absorption maxima of methylthiocyclopentadienone (**7**) and thiofluorenone (**8**) are strongly redshifted and appear at 700 nm.

The more intense shorter-wavelength absorptions of unsaturated and aromatic thioketones are satisfactorily reproduced by $\pi \rightarrow \pi^*$ transitions. The results of the

Table 1. Vertical transition energies, ΔE , in electron volts and absorption wavelengths λ in nanometers of sulfur-organic compounds in the near-ultraviolet and visible regions calculated by time-dependent density functional theory (TDDFT) (B3LYP/6-31+G*), by Zerner's semiempirical intermediate neglect of differential overlap (ZINDO)/S method (all valence electron approximation) and by the Pariser–Parr–Pople (PPP) method (π approximation) and experimental absorption wavelengths, λ_{\max} , at the absorption maxima. The symmetries in the *first column* refer to

the results of the TDDFT calculations. The order of the transitions calculated by semiempirical calculations were changed if different in symmetry. Kasha's classification of transitions in terms of $n \rightarrow \pi^*$, $\pi \rightarrow \pi^*$ single-electron excitation is less appropriate for not strictly planar compounds. Assignments of transitions given for some nonplanar compounds are approximate. Results of PPP calculations of conjugated compounds are missing for nonplanar compounds and planar compounds with hypervalent sulfur

Compound/symmetry (assignment)	TDDFT		ZINDO/S	PPP	Experiment	Reference
	ΔE	λ (f)	λ (f)	λ (f)	λ_{\max} (log ϵ)	
Thioacetone (1)						
A ₂ n \rightarrow π^*	2.53	490 (0.00)	527 (0.00)	–	532 (0–0)	[92] ^a
B ₂ n \rightarrow σ^*	5.28	235 (0.06)	218 (<0.01)	–	226 (0–0)	
A ₁ $\pi \rightarrow \pi^*$	5.73	217 (0.22)	239 (0.37)	220		
Thiocamphor (2)						
A n \rightarrow π^*	2.55	487 (0.00)	501 (<0.01)	–	493 (1.09)	[44] ^b
A n \rightarrow σ^*	5.10	243 (0.01)	225 (0.39)	–	244 (4.06)	
A $\pi \rightarrow \pi^*$	5.30	234 (0.22)	217 (0.01)	–	214 (3.62)	
Thioacrolein (3)						
A'' n \rightarrow π^*	2.07	598 (0.00)	624 (<0.01)	–	580	[93, 94] ^c
A' $\pi \rightarrow \pi^*$	4.80	258 (0.52)	276 (0.78)	269 (1.05)	275	
3-Methylthiocyclopentenone (4)						
A'' n \rightarrow π^*	2.29	541(0.00)	554 (0.0)	–	569 (1.31)	[95] ^d
A' $\pi \rightarrow \pi^*$	4.49	276 (0.51)	284 (0.74)	–	293 (4.22)	
A' $\pi \rightarrow \pi^*$	5.03	246 (0.04)	–	–		
A'' $\sigma \rightarrow \pi^*$	5.09	243 (<0.01)	–	–		
A' $\pi \rightarrow \pi^*$	5.52	224 (0.06)	215 (<0.01)	–	222 (3.5)	
Thiobenzaldehyde (5)						
A'' n \rightarrow π^*	2.10	590 (0.00)	618 (<0.01)	–	575	[93] ^c
A' $\pi \rightarrow \pi^*$	3.98	311 (0.06)	294 (0.50)	302 (0.79)	320	
A' $\pi \rightarrow \pi^*$	4.15	299 (0.39)	290 (0.31)	296 (0.11)		
1,1,3-Trimethylene-1,2-dihydrothionaphthalenone (6)						
A'' n \rightarrow π^*	2.02	614 (<0.01)	623 (<0.01)	–	618 (1.3)	[96] ^b
A' $\pi \rightarrow \pi^*$	3.36	369 (0.35)	350 (0.75)	–	376 (4.38)	
A'' $\pi \rightarrow \pi^*$	3.79	326 (0.03)	298 (0.07)	–	262 (4.05)	
3-Methylthiocyclopentadienone (7)						
A'' n \rightarrow π^*	1.63	762 (0.0)	750 (<0.01)	–	750	[94] ^c
A' $\pi \rightarrow \pi^*$	2.17	573 (<0.01)	495 (0.01)	–	450	
A' $\pi \rightarrow \pi^*$	4.52	274 (0.42)	277 (0.63)	–	320	
Thiofluorenone (8)						
A ₂ n \rightarrow π^*	1.86	666 (0.00)	673 (0.0)	–	700 (1.22)	[97] ^b
B ₂ $\pi \rightarrow \pi^*$	2.46	504 (0.00)	423 (<0.01)	414 (0.01)	428 (2.39)	
B ₂ $\pi \rightarrow \pi^*$	3.51	353 (0.08)	315 (0.03)	325 (0.13)		
A ₁ $\pi \rightarrow \pi^*$	3.63	342 (0.20)	313 (0.32)	341 (0.56)	344 (4.23)	
A ₂ $\pi \rightarrow \sigma^*$	4.10	302 (0.00)	–	–		
A ₁ $\pi \rightarrow \pi^*$	4.38	283 (0.08)	274 (0.42)	–		
B ₂ $\pi \rightarrow \pi^*$	4.77	260 (0.61)	253 (1.29)	282 (0.31)	270 (4.76)	
Thiotropone (9)						
A ₂ n \rightarrow π^*	2.12	584 (0.00)	600 (0.00)	–	610 (1.67)	[98] ^b
B ₁ $\pi \rightarrow \sigma^*$	2.18	570 (<0.01)	359 (<0.01)	–		
B ₂ $\pi \rightarrow \pi^*$	2.64	470 (0.01)	389 (0.05)	462 (0.02)		
A ₁ $\pi \rightarrow \pi^*$	3.71	335 (0.37)	355 (0.60)	347 (0.83)	371 (4.20)	
B ₂ $\pi \rightarrow \pi^*$	4.80	258 (<0.01)	221 (<0.01)	234 (0.00)		
B ₁ $\pi \rightarrow \sigma^*$	5.01	248 (<0.01)	232 (<0.01)	–		
A ₁ $\sigma \rightarrow \sigma^*$	5.39	230 (0.03)	222 (0.03)	–		
B ₂ $\pi \rightarrow \pi^*$	5.40	230 (0.01)	–	–		
A ₁ $\pi \rightarrow \pi^*$	5.49	226 (0.32)	226 (0.33)	230 (0.54)	253 (3.99)	
4H-Thiopyran-4-thione (10)						
A ₂ n \rightarrow π^*	2.15	577 (0.00)	642 (0.0)	–	588 (1.43)	[50] ^b
B ₁ $\sigma \rightarrow \pi^*$	3.52	352 (<0.01)	241 (<0.01)	–		
A ₁ $\pi \rightarrow \pi^*$	3.85	322 (0.45)	323 (0.75)	342 (1.13)	371 (4.32)	

Table 1. (Contd.)

Compound/symmetry (assignment)	TDDFT		ZINDO/S	PPP	Experiment	Reference
	ΔE	λ (f)	λ (f)	λ (f)	λ_{\max} (log ϵ)	
B ₂ $\pi \rightarrow \pi^*$	3.93	316 (<0.01)	255 (0.07)	327 (0.01)		
B ₂ $\pi \rightarrow \pi^*$	4.94	251 (0.01)	252 (0.11)	240 (0.08)	241 (3.34)	
2H-Thiopyran-2-thione (11)						
A'' n $\rightarrow\pi^*$	2.30	538 (<0.01)	613 (0.00)	–	587 (1.8)	[50] ^b
A' $\pi \rightarrow \pi^*$	3.10	400 (0.09)	356 (0.51)	385 (0.34)	433 (3.70)	
A'' $\sigma \rightarrow \pi^*$	3.70	335 (<0.01)	250 (<0.01)	–		
A' $\pi \rightarrow \pi^*$	4.28	290 (0.16)	257 (0.11)	296 (0.42)	318 (4.05)	
A' $\pi \rightarrow \sigma^*$	5.11	243 (<0.01)	246 (0.01)	–		
A' $\pi \rightarrow \pi^*$	5.17	240 (<0.01)	238 (0.02)	235 (0.05)	240 (4.07)	
1,2-Dithiole-3-thione (12)						
A'' n $\rightarrow\pi^*$	2.51	495 (<0.01)	607 (<0.01)	–	531 (1.91)	[51] ^b
A'' $\sigma \rightarrow \pi^*$	3.05	407 (0.00)	< 240	–	415 (3.83)	
A' $\pi \rightarrow \pi^*$	3.10	400 (0.02)				
A' $\pi \rightarrow \pi^*$	3.81	325 (0.23)	308 (0.59)	350 (0.81)	336 (3.80)	
A'' $\pi \rightarrow \sigma^*$	4.67	266 (0.00)	< 240	–		
A'' $\pi \rightarrow \sigma^*$	4.89	254 (0.00)	< 240	–		
A' $\pi \rightarrow \pi^*$	4.97	249 (0.10)	241 (0.02)	251 (0.14)	251 (3.92)	
Dimethylsulfide (13)						
A ₂	5.10	243 (0.00)	< 200	–		
B ₁	5.38	230 (<0.01)		–		
B ₁	5.95	210 (0.03)		–	203	[53] ^a
Thietane (14)						
A''	4.32	287 (0.00)	< 200	–	262 (1.54)	[99] ^t
Methylvinylsulfide (15)						
A''	4.95	250 (<0.01)		–		
A''	5.55	223 (<0.01)		–		
A' $\pi \rightarrow \pi^*$	5.58	222 (0.26)	< 200	–	225 (4.2)	[100] ^f
Thiete (16)						
A''	4.09	303 (0.00)	< 210	–	285 (1.70)	[101] ^g
A' $\pi \rightarrow \pi^*$	5.31	233 (0.09)	215 (0.24)	–	236 (3.48)	
A'	5.46	227 (<0.01)	< 210	–	215 (3.28)	
	5.51	225 (0.03)	< 210	–		
4H-Thiopyrane (17)						
A'' $\pi \rightarrow \pi^*$	4.29	289 (0.03)	227 (<0.01)	–	278 (3.39)	[102] ^h
A'	4.83	256 (<0.01)	212 (0.07)			
Thiophene (18)						
B ₂ $\pi \rightarrow \pi^*$	5.70	210 (0.10)	261 (0.20)	227 (0.21)	230	[103] ⁱ
B ₁ $\pi \rightarrow \sigma^*$	5.80	214 (0.09)	210 (0.01)	–		
A ₁ $\pi \rightarrow \pi^*$	5.97	208 (<0.01)	226 (0.02)	212 (0.34)	207	
Thieno[3,2-<i>b</i>]thiophene (19)						
B _u $\pi \rightarrow \pi^*$	4.76	260 (0.27)	305 (0.45)	264 (0.46)	259 (3.37)	[104] ^f
Benzthiet (20)						
A''	4.13	300 (0.00)	< 210	–		
A' $\pi \rightarrow \pi^*$	4.57	271 (0.03)	276 (0.01)	–	288 (3.26)	[105] ^d
A' $\pi \rightarrow \pi^*$	5.14	241 (0.15)	224 (0.11)	–	242 (4.07)	
Thiophenol (21)						
A'' $\pi \rightarrow \sigma^*$	4.73	262 (<0.01)		–		
A' $\pi \rightarrow \pi^*$	4.77	260 (0.01)	271 (<0.01)	300 (0.12)	281 (2.79)	[105] ^j
A' $\pi \rightarrow \pi^*$	5.19	239 (0.22)	219 (0.16)	269 (0.33)	236 (3.92)	
Benzo[<i>b</i>]thiophene (22)						
A' $\pi \rightarrow \pi^*$	4.61	269 (0.06)	292 (<0.01)	287 (0.07)	298 (3.81)	[106] ^{b,k}
A' $\pi \rightarrow \pi^*$	4.82	257 (0.02)	260 (0.43)	259 (0.13)	257 (4.05)	
A''	5.06	245 (0.00)	215 (<0.01)			
A' $\pi \rightarrow \pi^*$	5.45	227 (0.26)	222 (0.31)	226 (0.88)	226 (4.41)	
Benzo[<i>c</i>]thiophene (23)						
B ₂ $\pi \rightarrow \pi^*$	3.66	339 (0.07)	359 (0.28)	311 (0.31)	303 (4.06)	[107] ^{j,k}
A ₁ $\pi \rightarrow \pi^*$	4.61	269 (0.08)	290 (<0.01)	280 (0.14)	290 (3.97)	

Table 1. (Contd.)

Compound/symmetry (assignment)	TDDFT		ZINDO/S	PPP	Experiment	Reference
	ΔE	λ (f)	λ (f)	λ (f)	λ_{\max} (log ϵ)	
B ₁ $\pi \rightarrow \sigma^*$	4.90	253 (<0.01)	248 (<0.01)	–		
A ₂ $\pi \rightarrow \sigma^*$	5.01	247 (0.00)		–		
B ₂ $\pi \rightarrow \pi^*$	5.10	243 (<0.01)	257 (<0.01)	231 (0.04)		
A ₂ $\pi \rightarrow \sigma^*$	5.37	231 (0.00)	225 (0.00)	–		
B ₁ $\pi \rightarrow \sigma^*$	5.45	227 (<0.01)		–		
B ₂ $\pi \rightarrow \pi^*$	5.72	217 (<0.01)		–		
A ₂ $\pi \rightarrow \sigma^*$	5.77	215 (<0.01)		–		
A ₁ $\pi \rightarrow \pi^*$	5.92	209 (0.17)	222 (1.52)	215 (1.49)	215 (4.84)	
2,2'-Bisthiophene (24)						
B	3.98	311 (0.05)	326 (0.76)	290 (0.82)	301 (3.88)	[108] ^d
A	4.88	254 (<0.01)	259 (0.01)	–		
A	4.91	252 (0.00)	257 (<0.01)	–		
B	5.06	245 (0.01)	237 (0.03)	247 (0.01)		
B	5.12	242 (0.03)	233 (0.01)	230 (0.40)	249 (4.14)	
Cyclopenta[<i>b</i>]thiapyran (25)						
A' $\pi \rightarrow \pi^*$	2.40	516 (0.01)	460 (0.04)	484 (0.10)	537 (2.82)	[109] ^{b,k}
A' $\pi \rightarrow \pi^*$	3.80	326 (0.13)	335 (0.42)	325 (0.31)	350 (3.76)	
A'' $\pi \rightarrow \sigma^*$	4.71	264 (<0.01)		–		
A'' $\pi \rightarrow \sigma^*$	4.76	260 (<0.01)	245 (<0.01)	–		
A' $\pi \rightarrow \pi^*$	5.09	244 (0.40)	238 (0.12)	247 (0.35)	268 (4.08)	
Cyclopenta[<i>c</i>]thiapyran (26)						
A' $\pi \rightarrow \pi^*$	2.86	433 (0.03)	437 (0.10)	428 (0.15)	465 (3.08)	[110] ^{d,k}
A' $\pi \rightarrow \pi^*$	3.96	313 (0.02)	310 (0.08)	316 (0.11)	329 (3.38)	
A'' $\pi \rightarrow \sigma^*$	4.69	264 (0.00)		–		
A'' $\pi \rightarrow \sigma^*$	4.80	258 (<0.01)		–		
A' $\pi \rightarrow \pi^*$	4.86	255 (0.40)	255 (0.75)	261 (0.74)	273 (4.34)	
A' $\pi \rightarrow \sigma^*$	5.15	241 (<0.01)	238 (<0.01)	–		
A' $\pi \rightarrow \sigma^*$	5.26	236 (<0.01)	222 (<0.01)	–		
A' $\pi \rightarrow \pi^*$	5.43	228 (0.51)	218 (0.36)	225 (0.42)	257 (4.28)	
1-Thiaphenylene (27)						
A' $\pi \rightarrow \pi^*$	3.16	392 (0.08)	341 (0.06)	356 (0.20)	407 (3.43)	[111] ^f
A' $\pi \rightarrow \pi^*$	3.61	342 (0.09)	323 (0.37)	334 (0.42)	357 (3.93)	
A' $\pi \rightarrow \pi^*$	3.98	312 (0.05)	279 (<0.01)	307 (0.11)		
A' $\pi \rightarrow \pi^*$	5.00	247 (0.19)	239 (0.88)	244 (0.64)	248 (4.26)	
Thieno[3,4-<i>d</i>]thiopyne (28)						
B ₂ $\pi \rightarrow \pi^*$	3.00	413 (<0.01)	280 (0.01)	368 (0.01)	378 (2.49)	[112] ^{j,k}
A ₁ $\pi \rightarrow \pi^*$	3.81	325 (0.07)	289 (0.09)	303 (0.36)	318 (3.30)	
B ₁ $\pi \rightarrow \sigma^*$	4.50	276 (<0.01)	233 (0.01)	–		
A ₂ $\pi \rightarrow \sigma^*$	4.56	272 (0.00)	225 (0.01)	–		
A ₂ $\pi \rightarrow \sigma^*$	4.82	257 (0.00)		–		
A ₁ $\pi \rightarrow \pi^*$	5.00	248 (0.51)	230 (1.48)	232 (1.12)	260 (4.41)	
Tetrathiofulvalene (29)						
A ₁	2.65	468 (<0.01)		320 (0.00)	450 (2.43)	[113] ^b
B ₂ $\pi \rightarrow \pi^*$	3.37	368 (0.02)	292 (<0.01)	316 (0.20)	368 (3.28)	
B ₁ $\pi \rightarrow \pi^*$	3.81	326 (0.02)	232 (0.19)	285 (0.61)	303 (4.11)	
4,4'-Bithiopyrylene (30)						
A _u $\sigma \rightarrow \pi^*$	2.63	471 (<0.01)		–		
B _{1g} $\sigma \rightarrow \pi^*$	3.27	378 (0.0)		–		
B _{1u} $\pi \rightarrow \pi^*$	3.28	378 (0.95)	363 (1.47)	393 (1.66)	387 (4.74)	[114] ^l
2,6-Bis-<i>tert</i>-butylthiopyne (31)						
A''	3.09	402 (0.01)	289 (0.18)	–	362 (2.51)	[115] ^b
A''	4.50	275 (0.04)		–	252 (3.35)	
A'	4.72	263 (0.01)	245 (0.01)	–		
A'	4.88	254 (<0.01)	238 (0.04)	–		
A'	5.18	239 (0.01)	227 (0.04)	–		
A'	5.30	234 (0.02)		–		
A'	5.33	233 (<0.01)	209 (0.03)	–		
A'	5.49	226 (0.07)		–		
A'	5.54	224 (0.10)	227 (0.04)	–	226 (4.02)	

Table 1. (Contd.)

Compound/symmetry (assignment)	TDDFT		ZINDO/S	PPP	Experiment λ_{\max} (log ϵ)	Reference
	ΔE	λ (f)	λ (f)	λ (f)		
1,4-Dithiin (32)						
A ₂	3.59	345 (0.00)	223 (0.00)	–		
B ₂	4.83	257 (0.09)	219 (0.07)	–	262 (3.73)	[116] ^f
1,2-Dithiin (33)						
B	2.37	523 (<0.01)	262 (0.21)	–	450 (1.95)	[117] ^m
A	4.32	287 (0.03)	215 (<0.01)	–	279 (3.30)	
B	4.33	286 (0.02)	215 (0.02)	–	248 (3.18)	
Dimethyl disulfide (34)						
B n→σ*	4.57	271 (0.01)	<200	–	256 (2.54)	[118] ⁱ
1,2-Dithiane (35)						
B n→σ*	3.91	317 (<0.01)	<200	–	290 (2.49)	[119] ^h
Naphtho[1,8-<i>cd</i>]dithiol (36)						
B ₁ π→σ*	2.35	527 (<0.01)			480 (1.85)	[62] ⁿ
A ₁ π→π*	3.49	355 (0.17)	292 (0.25)	347 (0.48)	371 (4.18)	
B ₂ π→π*	3.76	330 (0.04)	325 (0.25)	351 (0.10)	357 (4.08)	
A ₂ π→σ*	4.04	307 (0.00)	233 (0.00)	–		
A ₂ π→σ*	4.42	281 (0.00)				
A ₂ π→σ*	4.53	274 (0.00)				
B ₁ π→σ*	4.60	270 (<0.01)				
B ₂ π→π*	4.63	268 (<0.01)	234 (0.25)	269 (<0.01)		
A ₂ π→σ*	4.72	262 (0.00)				
B ₁ π→σ*	5.02	247 (<0.01)				
B ₂ π→π*	5.14	241 (0.19)	228 (1.13)	247 (0.52)	253 (4.42)	
1,6,6aλ⁴-Trithiapentalene (37)						
B ₁ σ→π*	2.67	464 (0.0)	933 (<0.01)			
B ₂ π→π*	2.79	445 (0.03)	483 (0.13)	–	472 (3.68)	[120] ^b
B ₁ π→σ*	3.27	379 (<0.01)	236 (<0.01)	–		
A ₁ π→π*	4.48	277 (0.00)	270 (0.17)	–		
A ₁ π→π*	4.70	264 (0.03)	244 (0.03)	–		
B ₂ π→π*	5.30	234 (1.27)	203 (0.68)	–	254 (4.69)	
1,2-Dithiolylium (38)						
B ₂ π→π*	4.78	259 (0.01)	296 (0.23)	282 (0.41)	288 (3.59)	[121] ^o
A ₂ σ→π*	4.91	253 (0.00)		–		
B ₁ σ→π*	5.19	239 (<0.01)		–		
A ₁ π→π*	5.40	230 (0.02)	251 (0.19)	246 (0.50)	245 (3.62)	
1,3-Dithiolylium (39)						
A ₁ π→π*	4.92	252 (0.06)	348 (0.10)	269 (0.24)	254 (3.58)	[121] ^o
B ₂ π→π*	5.67	219 (0.09)	241 (0.09)	243 (0.35)	212 (3.58)	
Thiopyrylium (40)						
B ₂ π→π*	4.89	254 (0.06)	301 (0.26)	289 (0.18)	284 (3.54)	[122] ^l
A ₁ π→π*	5.44	228 (0.08)	234 (0.20)	244 (0.3329)	245 (3.76)	
2-Benzothiopyrylium (41)						
A' π→π*	3.20	387 (0.06)	409 (0.22)	395 (0.21)	~380 (3.6)	[123] ^p
A' π→π*	4.14	300 (0.02)	296 (0.06)	317 (0.16)	~310 (3.7)	
A' π→π*	5.11	243 (0.29)	243 (0.35)	255 (0.16)		
A' π→π*	5.29	235 (0.29)	239 (0.52)	247 (0.86)	~255 (4.6)	
Methylmercaptotropylium (42)						
A' π→π*	3.14	395 (0.02)	276 (0.04)	317 (0.01)		
A' π→π*	3.75	330 (0.29)	296 (0.23)	402 (0.42)	378 (4.24)	[124] ^l
A' π→π*	5.19	239 (0.02)	222 (0.32)	256 (0.47)	258 (4.17)	
3,4-Dimethylenethiophene (43)						
B π→π*	1.90	651 (0.09)	617 (0.40)	509 (0.49)	572 (3.71)	[65] ⁿ
Adamantanethione S-methylide (44)						
A'		402 (<0.01)		[125] ^q		
A'	3.67	338 (0.34)	351 (0.93)		350	
Thiosulfine (45)						
A' n→π*	2.39	518 (0.00)	912 (<0.01)		~500	[69] ^q
A' π→π*	3.72	333 (0.17)	487 (0.29)		356	

Table 1. (Contd.)

Compound/symmetry (assignment)	TDDFT		ZINDO/S	PPP	Experiment	Reference
	ΔE	λ (f)	λ (f)	λ (f)	λ_{\max} (log ϵ)	
Thieno[3,4- <i>c</i>]thiophene (46)						
$B_{2u} \pi \rightarrow \pi^*$	2.82	439 (0.08)	568 (0.34)	416 (0.47)	553 (4.11)	[126] ^{m,r}
Acenaphtho[3,6- <i>cd</i>]thiopyran (47)						
$B_2 \pi \rightarrow \pi^*$	2.18	569 (0.04)	696 (0.14)	632 (0.12)	565 (3.59)*	[127] ^{m,r}
Thieno[3,4- <i>f</i>]isothianaphthene (48)						
$B_{2u} \pi \rightarrow \pi^*$	1.95	637 (0.05)	677 (0.34)	534 (0.41)	793 (4.06)	[128] ^s
$B_{3g} \pi \rightarrow \pi^*$	3.38	367 (0.00)	436 (0.00)	370 (0.00)		
$B_{3g} \pi \rightarrow \pi^*$	3.95	314 (0.00)	369 (0.01)	343 (0.20)		
$B_{1u} \pi \rightarrow \pi^*$	3.97	312 (0.25)	356 (0.00)	324 (0.00)	316 (4.38)	
<i>S</i> -Methylthiophenium (49)						
A''	4.49	276 (0.03)	240 (0.23)		267 (2.85)	[129] ^t
$A' \pi \rightarrow \pi^*$	5.70	218 (<0.01)	217 (<0.01)			
$A' \pi \rightarrow \pi^*$	5.97	208 (0.10)	209 (0.03)		220 (3.32)	
Thiophene <i>S</i> -dioxide (50)						
$B_2 \pi \rightarrow \pi^*$	4.06	305 (0.02)	304 (0.02)		289 (2.94)	[130] ^j
A_2	4.43	280 (0.00)	321 (0.00)			
A_1	4.96	250 (0.05)			220 (3.30)	
B_1	5.65	219 (0.01)	276 (<0.01)			

^a Gas phase^b In cyclohexane^c On sodium chloride at about 77 K^d In hexane^e In alcohol glass at 77 K^f In ethanol^g In 2,2,4-trimethylpentane^h In heptaneⁱ In petrolether^j In methanol^k Absorption band with a pronounced vibrational fine structure^l In acetonitrile^m In methylene chlorideⁿ In methylcyclohexane^o In acidic ethanol^p In acetic acid^q In argon at 10 K^r The theoretical calculation did not consider phenyl substituents^s In chloroform^t In isoctane

TDDFT calculations are very close to those of semiempirical calculations. Polarization measurements are reported for thiofluorene [49]. The maxima of the first two bands at about 430 and 340 nm are long- and short-axis polarized, respectively ($B_2 \leftarrow A_1$ and $A_1 \leftarrow A_1$ transitions, respectively). In agreement with experiment the most intense transition of the NUV at about 270 nm is long-axis polarized ($B_2 \leftarrow A_1$ transition). The two intense $\pi \rightarrow \pi^*$ transitions ($B_2 \leftarrow A_1$) of thiotropone (**9**) are less well calculated. Although the thiopyronthiones **10** and **11** are both isoconjugate with **9**, the spectra are characteristically different both according to theory and to experiment. This fact was already discussed at the PPP level [50]. A more interesting case is encountered with 1,2-dithiole-3-thione (**12**). The spectrum of this compound was not well understood at semiempirical levels of theory [51, 52] including the ZINDO/S method. Using a modified CNDO procedure Pfister-Guillouzo et al. [52] calculated an $n \rightarrow \sigma^*$ transition in the long-wavelength part of the spectrum. The TDDFT calculation suggests that the first intense absorption of **12** at about 400 nm is a mixed $n(S) \rightarrow \sigma^*(SS)/\pi \rightarrow \pi^*$ transition. In addition, there is a low-energy transition of $\pi \rightarrow \sigma_{SS}^*$ character of lower transition probability. The Kohn–Sham orbitals involved in the lowest-energy one-electron transitions of **12** are illustrated in Fig. 1.

3.2 Compounds with dicoordinated and higher-coordinated sulfur

The calculated spectral data of the two saturated sulfides **13** and **14** with weak electronic transitions in the short-wavelength NUV region are compared with experimental data in Table 1. Dimethyl sulfide (**13**) shows a non-Rydberg-type transition at about 200 nm [53]. According to DFT calculations this absorption is due to an $n \rightarrow \sigma^*$ transition. Forbidden transitions may cause a tail of the absorption band at longer wavelengths. The TDDFT calculation of **13** predicts a localized $p_z \rightarrow p_x^*$ transition at the lowest energy such as found earlier in CNDO calculations [54]. The molecular orbitals (MOs) (atomic orbitals) of this one-electron transition are depicted in Fig. 1. The redshift in passing from dimethyl sulfide (**13**) to thietane (**14**) is underestimated by TDDFT. Because Rydberg-type absorption bands may occur in this spectral region, TDDFT assignment of the high-energy NUV absorptions of saturated sulfides is less certain when Rydberg functions are not included in the basis set. According to the ZINDO/S calculations of **13** and **14** there is no valence-type transition larger than 200 nm (cf. Table 1).

If dicoordinated sulfur is involved in a conjugated system, the transitions are found and calculated at longer wavelengths and the spectral data are more

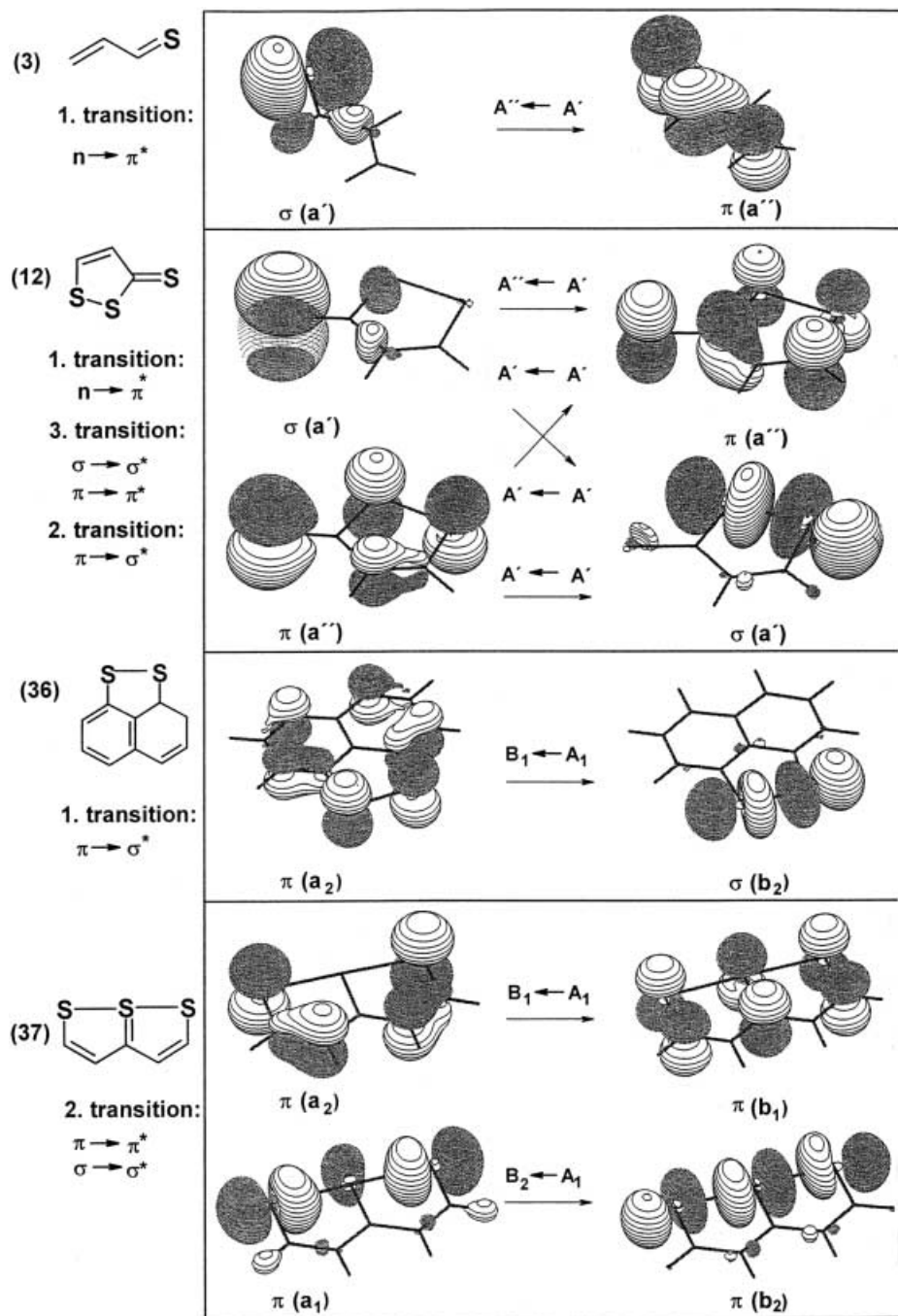
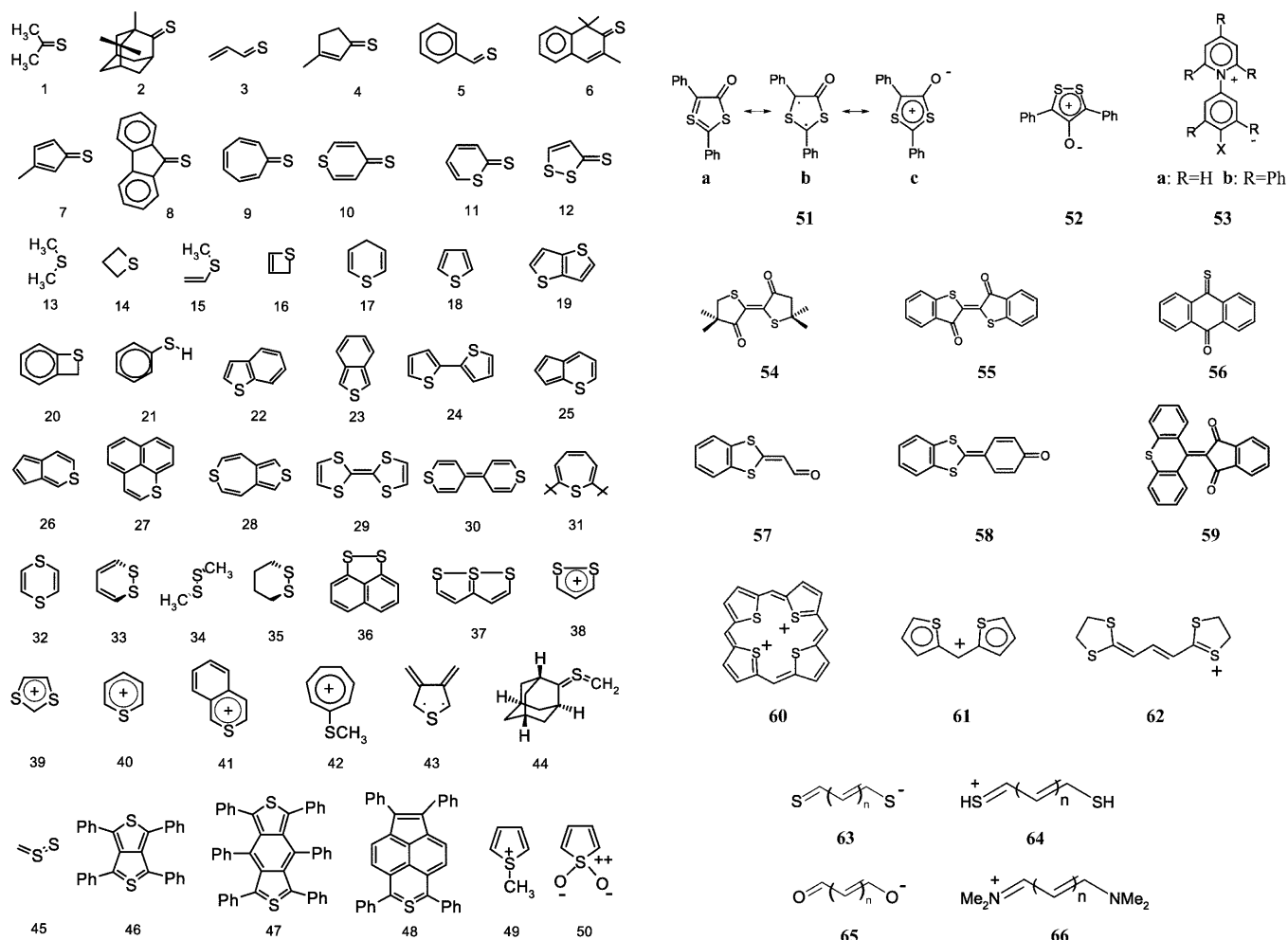


Fig. 1. Interpretation of selected low-energy electron transitions in terms of the predominant one-electron transitions between Kohn-Sham orbitals (visualization using the MOLDEN program)

informative. The longest-wavelength absorptions of the simplest unsaturated compounds, methylvinylsulfide (**15**) and thiete (**16**), are reasonably well reproduced. They originate in $\pi \rightarrow \pi^*$ transitions. According to both theory and experiment the first absorption band of 4*H*-thiopyran (**17**) is significantly bathochromically shifted relative to **15**. While 4*H*-thiopyran (**17**), thiophene (**18**) and thieno[3,2-*b*]thiophene (**19**) absorb at short wavelengths in the NUV, substituted benzenes, such as **20** and **21**, and annelated thiophenes, such as benzo[*b*]thiophene (**22**) and benzo[*c*]thiophene (**23**), and 2,2-bisthiophene (**24**), display the first absorption band at more than 300 nm. As shown in Table 1 these characteristics

are well reproduced by TDDFT calculations. The calculated lowest-energy electron transition of thiophenol (**21**) is unexpected. It is due to an almost forbidden $n \rightarrow \sigma^*(SH)$ -type transition (Fig. 1) that may be hidden beneath the first $\pi \rightarrow \pi^*$ absorption band. The absorption spectrum of **21** is essentially understood at the π level of theory [37]. In contrast to the benzothiophenes **22** and **23** the isomeric cyclopentathiopyrans **25** and **26** are colored compounds. The results of the TDDFT calculations reflect not only the shape of the spectrum but also the bathochromic shifts. Thus, benzo[*c*]thiophene (**23**) is correctly predicted to be redshifted relative to benzo[*b*]thiophene (**22**) and cyclopenta[*c*]thiopyrane (**26**) is



predicted to be redshifted relative to cyclopenta[*b*]thiopyran (**25**). As documented in Table 1, these characteristics are also found by PPP calculations. Whereas thieno[3,2-*b*]thiophene (**19**) is colorless, thieno[3,4-*d*]thiepin (**28**) is yellow. The TDDFT calculation also confirmed that a weak $\pi \rightarrow \pi^*$ transition of 1-thiaphenylene (**27**) gives rise to the weak long-wavelength absorption band at about 400 nm. The intense band of **27** is expected and found at about 250 nm. A low-intensity $\pi \rightarrow \pi^*$ TDDFT transition causes the weak absorption of thieno[3,4-*d*]thiepin (**28**) observed in the 400 nm region. Gleiter et al. [55] performed polarization measurements of **28** in stretched films. TDDFT is in agreement with the experimental outcome that the long-wavelength color-determining transition is polarized along the short axis ($B_2 \leftarrow A_1$ transition) followed by a long-axis polarized transition ($A_1 \leftarrow A_1$ transition). The intense shorter-wavelength absorption is again polarized parallel to the twofold axis. Geometry optimization of tetrathiofulvalene (**29**) resulted in a slightly out-of-plane bent structure of C_s symmetry rather than the expected planar structure (D_{2h}). A nonplanar boat structure was also found by an ab initio calculation [56] and was verified in an electron diffraction study of this compound [57]. The first electronic transition is forbidden in D_{2h} symmetry and nearly forbidden in C_{2v} symmetry. Whereas the TDDFT

calculation reproduces the long-wavelength absorption reasonably well, semiempirical calculations provide this transition at wavelengths much too short. The short-axis polarized next transition of $B_2 \leftarrow A_1$ symmetry is of low intensity followed by a long-axis polarized $B_1 \leftarrow A_1$ transition. These results are in agreement with polarization measurements [58] for the more intense transitions mentioned last. In contrast to **29** 4,4'-bis-thiopyrylene (**30**) was calculated to be planar. Steric

strain is obviously released by extension of the central CC bond (1.40 Å). According both to theory and to experiment the first intense absorption is placed at about 300 nm. The transition was calculated and measured to be remarkably intense by theory and experiment ($f = 0.95$ and $\log \epsilon = 4.74$, respectively).

2,6-Bis-*tert*-butylthiopin (**31**) is a molecule of boatlike shape. The weak electron transition calculated at 400 nm is polarized perpendicular to the twofold axis. The lowest-energy transition is mainly caused by an electronic transition from a localized orbital of sulfur to the antisymmetric delocalized MO. This MO consists of local two-center π bonds that overlap to a delocalized " $\tilde{\pi}$ bond" system in the nonplanar structure. Thus, the transition might be tentatively denoted as $n \rightarrow \tilde{\pi}^*$. This transition obviously corresponds to the intense absorption band recorded at about 360 nm [59]. The intense transition of the short-wavelength absorption at 230 nm is polarized in the molecular plane of the molecule. According to magnetic circular dichroism measurements there are two additional transitions which obviously contribute to the long-wavelength tail of the first absorption band. The origin of these transitions is not clear. Formal replacement of a double bond of **31** by sulfur results in the colorless 1,4-dithiin (**32**) or the colored 1,2-dithiin (**33**). Like **31** the dithiin isomers are of puckered structure of different symmetry (Table 1). Again, TDDFT provided satisfactory results. As detailed elsewhere [29], the TDDFT study of **33** predicts $\tilde{\pi} \rightarrow \sigma^*$ and $\tilde{\pi} \rightarrow \tilde{\pi}^*$ type transitions which determine the NUV/vis spectrum. Although the CIS calculation of **31** resulted in a first absorption band at 350 nm rather than the 450 nm found experimentally [29, 60], the nature of the transition is the same as in TDDFT calculations [29].

As is well known the long wavelength absorptions of saturated disulfides such as **34** and **35** are of the $n \rightarrow \sigma^*$ type. A prototype $\pi \rightarrow \sigma^*$ transition is calculated for the planar naphtho[1,8-*cd*]dithiole (**36**). The relevant MOs of this transition are depicted in Fig. 1. This calculation confirmed an early tentative assignment of the color band of **36** [61, 62]. However, the color band of 1,6,6a λ^4 -trithiapentalene (**37**) with a formal central hypervalent sulfur atom is of different origin. As found by Spanget-Larsen et al. [63] by AM1-CI and CIS calculations, the first intense transition is of mixed $\pi \rightarrow \pi^*$ and $\sigma \rightarrow \sigma^*$ character. The σ and σ^* orbitals reflect the SSS three-center two-electron bond [63] (Fig. 1). According to the TDDFT calculations a forbidden $\sigma \rightarrow \pi^*$ transition is situated at nearly the same wavelengths as the previously mentioned first intense transition. As expected by TDDFT the measured linear dichroism of the weak color-determining band at about 470 nm and the shorter-wavelength intense absorption at about 250 nm are long-axis polarized. A short-axis polarized intense transition was rather expected in first-order CI calculations [64].

The UV spectra of the 6π -sulfur-heterocyclic cations 1,2-dithiolylium (**38**), 1,3-dithiolylium (**39**), thiopyrylium (**40**) and 2-benzothiopyrylium (**41**) have well-separated absorption bands. This facilitates the comparison between theoretical and experimental results. Although protic or polar solvents may affect the experimental

data, the agreement between theory and experiment is very satisfactory. The solvent effect may be not negligible for methylmercaptotropylium (**42**). The TDDFT calculation overestimated the intense lowest-energy transition energy by 0.48 eV, with respect to the experimental absorption band measured in acetonitrile. The position of the color band, however, was surprisingly well predicted by PPP [39] (Table 1).

Finally the spectral data of some compounds which formally contain tetravalent sulfur are discussed. Alternatively the structures may be written as diradicals, such as in the case of 3,4-dimethylenethiophene (**43**) [65], or as ylides, such as in the case of the compounds adamantanthione *S*-methylide (**44**) [66], thiosulfine (**45**) [67] and the heterocycles **46–48** [66]. To avoid lengthy formula descriptions, we adhere to the hypervalent structure of the sulfur. A simple chromophore of this type is the matrix-isolated **44** with a local 4π system. In agreement with the TDDFT calculations this compound absorbs at about 300 nm as found in a low-temperature matrix (Table 1). Whereas the CIS method normally predicts strongly blueshifted absorptions, the spectral absorptions of *S*-ylides are exceptionally well calculated in this approximation [68]. Sulfine (thioformaldehyde *S*-sulfide) contains the same type of 4π chromophore as **44** and the intense $\pi \rightarrow \pi^*$ absorption band is predicted in the same wavelength region. The recent successful matrix isolation of **45** by Młostoń et al. [69] supported the prediction. Whereas a former CIS calculation [67] predicted a weak long-wavelength absorption at 330 nm, the TDDFT calculations resulted in about 500 nm. According to experiment [69] the latter result is more realistic. As shown in Table 1, ZINDO/S did not reproduce the spectrum of **45**. Heterocyclic compounds with a formal hypervalent sulfur generally show long-wavelength absorptions, as exemplified by the fully phenyl substituted derivatives of the heterocycles thieno[3,4-*b*]thiophene (**46**), thieno[3,4-*f*]isothionaphthene (**47**) and acenaphtho[3,6-*cd*]thiopyran (**48**). These compounds absorb at considerably longer wavelengths than the heterocyclic isomers of conventional structure. Since the phenyl groups were not considered in the calculations, the position of the color bands is calculated at wavelengths too short. The *S*-methylated thiophene (**49**) and thiophene *S,S*-dioxide (**50**) are polar compounds with a tricoordinated or a tetracoordinated sulfur. In agreement with experiment the longest-wavelength absorption band is calculated at about 270 and 300 nm, respectively, and thus is considerably redshifted compared to the thiophene (**18**) parent compound (Table 1).

Although ZINDO/S calculations should predict all types of valence electron transitions there are unexpected limitations. Transitions of $n \rightarrow \sigma_{ss}^*$ type of aliphatic disulfides (**34**, **35**) and thiosulfine (**45**) and of $\pi \rightarrow \sigma_{ss}^*$ type of unsaturated disulfides (**33**, **36**) are not calculated to be in the wavelength region found experimentally. Also, the color of compounds **33** and **36** is not understood by ZINDO/S in the present parameterization. Some weakness of ZINDO/S is also indicated in the short-wavelength region of saturated sulfides. However, transitions of the type $n \rightarrow \pi^*$ and $\pi \rightarrow \pi^*$ are reasonably well calculated by ZINDO/S.

3.3 Performance of the methods

When evaluating the performance of TDDFT in calculating spectral absorption data three limiting factors should be addressed. Firstly, the vertical transition energies are, strictly speaking, not observables and the comparison of the calculated wavelengths with the experimental wavelengths at the absorption maxima is therefore approximate. Secondly, the positions of the experimental absorption maxima are affected by band overlap and the comparison is more difficult when vibrational fine structure occurs. Thirdly, the spectra discussed in this study are generally recorded in solvents. Polar and protic solvents will more or less affect the experimental absorption data.

Statistical analysis of the deviation of the calculated TDDFT transition energies from experiment was carried out for **1–50** as far as calculated and experimental data are clearly correlated. Not considered were data for **13** and **14** (not well-assigned high-energy electron transitions) and **42** (probably affected by solvatochromic effects). In the case of the ZINDO/S results all data were disregarded where the method obviously fails. The analysis of the ZINDO/S spectral data was actually confined to $\pi \rightarrow \pi^*$ and $n \rightarrow \pi^*$ type transitions. The experimental data for these transitions were compared with the TDDFT results. In the case of PPP, the comparison was restricted to $\pi \rightarrow \pi^*$ type transitions.

The consideration of 68 spectral data of different origin by TDDFT resulted in an absolute mean deviation of 0.21 eV ($n \rightarrow \pi^*$ 0.09 eV, $\pi \rightarrow \pi^*$ 0.22 eV). The deviation of ZINDO/S transition energies was calculated to be 0.35 eV ($n \rightarrow \pi^*$ 0.09 eV, $\pi \rightarrow \pi^*$ 0.40 eV). Stronger deviations between 0.8 and 1.3 eV were found in ZINDO/S calculations for **11**, **26**, **28** and **39**, contributing to the larger mean deviation of $\pi \rightarrow \pi^*$ excitation energies. In an attempt to improve the ZINDO/S results, the calculations for the whole series of compounds were repeated with consideration of all mono-excited configurations. The $n \rightarrow \pi^*$ excitation energies were found to be nearly unchanged. The results of the $\pi \rightarrow \pi^*$ excitation energies were slightly improved (mean deviation of 0.32 eV rather than 0.40 eV). The term level orders at the lowest energies were essentially the same as with the limited CI. In this approximation, however, the longest-wavelength absorptions of non-classical structures, such **43–48**, are in part strongly redshifted toward the NIR region (e.g. **47** and **48**). These absorption wavelengths are much in error or appear less realistic.

The average error of the PPP calculations ($\pi \rightarrow \pi^*$) amounts to 0.20 eV for the same $\pi \rightarrow \pi^*$ transition considered in TDDFT and ZINDO/S calculations (56 spectral data). The good success of the “old fashioned” PPP method is remarkable. Thus, the performance in calculating $\pi \rightarrow \pi^*$ transitions decreases in the order PPP > TDDFT > ZINDO/S. For $n \rightarrow \pi^*$ the error is comparable in TDDFT and ZINDO/S calculations (about 0.09 eV, 12 values).

Thus, the results of TDDFT calculations over a wide range of the spectral data of sulfur-organic compounds are not less accurate than those of parameterized

methods; however, in contrast to semiempirical methods, TDDFT can more satisfactorily cope with all types of valence electron transitions, providing the spectrum of the whole spectral region. This advantage is paid for by the higher price of computer time. The computer time will be reduced, however, with more efficient programs (e.g. by linear scaling). Nevertheless, in calculations of $n \rightarrow \pi^*$ and $\pi \rightarrow \pi^*$ transitions or only for $\pi \rightarrow \pi^*$ transitions the less expensive ZINDO/S and PPP methods, respectively, will remain attractive and their application is justified, to some extent, by the results of first-principles methods, such as TDDFT.

3.4 Selected chromophores and bichromophores

The good performance shown with the compounds **1–50** stimulated additional calculations of some more complex chromophoric systems, including those of fundamental dye chromophores which had so far been treated by semiempirical methods only. By paying attention only to electronic transitions that actually determine the spectral absorption features, the number of calculated data listed in Tables 2, 3 and 4 is reduced. A compound of seemingly ambiguous structure is exemplified by **51** in Table 2. As discussed for **44–48** a hypervalent (**51a**), a diradical (**51b**) or a charge-separated formula (**51c**) may be invoked. The last-mentioned “mesoionic” [70] formula presentation **51c** is generally preferred because of the potential aromatic 1,3-dithiolylium substructure. The same holds for **52** with a potential 1,2-dithiolylium substructure. Both compounds are deeply colored, absorbing at about 550 nm. To allow a direct comparison between experiment and theory, the two phenyl groups of **51** and **52** were considered in the geometry optimization (B3-LYP/6-31G*). These groups are tilted out of the heterocyclic ring plane (**51**: 23° in the 2-position and 15° in the 5-position, **52**: 20°, C_s symmetry). As shown in Table 2, the absorption wavelengths of the color bands of **51** as well as of **52** are very well reproduced by TDDFT. Both compounds display negative solvatochromism, suggesting a decrease in the dipole moment on excitation [71, 72]. The experimental dipole moment of **51** is about 5 D [71].

The extensively studied strongly polar pentaphenyl-substituted pyridino *N*-phenoxide betaine dyes (**53**, $R = \text{phenyl}$) with ground-state dipole moments larger than 10 D belong to the extremely solvatochromic compounds, with a solvatochromic range of more than 1 eV [73]. In less-polar solvents the phenyl-substituted dyes absorb in the NIR region. In the TDDFT calculations the five phenyl groups had to be neglected and the parent compounds were calculated instead. The parent compounds are twisted by about 30° (C_2 symmetry) [74]. Whereas the parent thioxide **53a** ($X = \text{O}$, $R = \text{H}$) is unknown, the oxide has recently been synthesized and measured spectroscopically [75]. Unfortunately, the parent pyridino *N*-phenoxide (**53a**, $X = \text{O}$, $R = \text{H}$) is not sufficiently soluble in nonpolar solvents. In consideration of the spectral data measured in the protic ethanol (413 nm) and the polar aprotic dimethyl sulfoxide (486 nm) and the estimated solvatochromic range, the compound should

Table 2. Calculated and experimental data relevant for the absorption characteristics of some sulfur-containing chromophores in nanometers (TDDFT, ZINDO/S in italics)

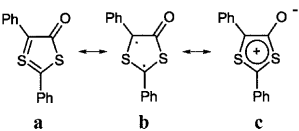
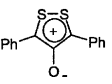
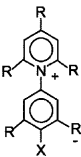
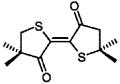
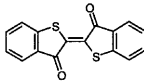
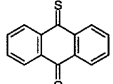
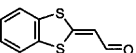
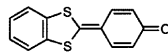
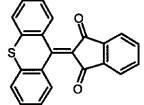
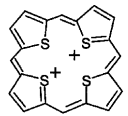
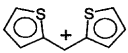
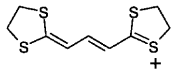
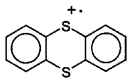
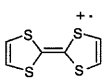
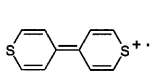
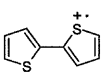
							
51		52		53			
TDDFT	Exp. ^{a)}	TDDFT	Exp. ^{b)}	R	X	TDDFT	Exp.
565 (0.34)	559 (-4.0)	585 (0.35)	575 (4.23)	H	S	584 (0.61)	–
705 (0.64)		565 (0.94)		H	O	497 (0.52)	~550
							
54		55		56			
TDDFT	Exp. ^{c)}	TDDFT	Exp. ^{d)}	TDDFT	Exp. ^{e)}		
472 (0.07)	450 (4.13)	508 (0.16)	~546 (4.2)	725 (0.0)	697 (1.67)		
294 (0.46)		311 (0.30)		777 (0.0)			
		325 (0.21)	~310 (4.2)	369 (0.12)	334 (4.16)		
		308 (0.11)		334 (0.31)			
		275 (0.18)	~280 (4.3)				
							
57		58		59			
TDDFT	Exp. ^{f)}	TDDFT	Exp. ^{g)}	TDDFT	Exp. ^{h)}		
321 (0.38)	372 (4.23)	384 (0.79)	450 (4.62)	468 (0.06)	440 (3.92)		
267 (0.57)		334 (1.26)		404 (0.01)			
				368 (0.13)	332 (4.15)		
				308 (0.57)			
							
60		61		62			
TDDFT	Exp. ⁱ⁾	TDDFT	Exp. ^{j)}	TDDFT	Exp. ^{k)}		
603 (<0.01)	646 (3.63)	419 (0.17)	487 (4.33)	425 (0.99)	548		
756 (0.01)	595 (3.91)	446 (1.14)		395 (1.22)			
603 (<0.01)		357 (0.53)	~375 (4.3)				
756 (0.01)		286 (0.28)					
493 (0.89)	456 (4.98)						
372 (1.42)							
493 (0.89)							
372 (1.42)							

Table 2. (Contd.)

							
67		68		69		70	
TDDFT	Exp. ^{d)}	TDDFT	Exp. ^{m)}	TDDFT	Exp. ⁿ⁾	TDDFT	Exp. ^{o)}
982 (<0.01)	~1050 (3.1)	504 (0.00)	579 (3.70)	787 (0.40)	726 (4.17)	549 (0.04)	590
531 (0.14)	~540 (4.2)	388 (<0.01)	434 (4.27)	330 (0.17)	451 (4.64)	374 (0.49)	425
280 (0.64)	~300 (4.8)	302 (0.05)	338 (3.78)				

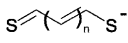
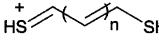
^{a)} in benzene, ref. 71 ^{b)} in benzene, ref. 72 ^{c)} in cyclohexane, ref. 77 ^{d)} in chloroform, ref. 77 ^{e)} in chloroform, ref. 131 ^{f)} in chloroform, ref. 132 ^{g)} in chloroform, ref. 133 ^{h)} solvent unknown, ref. 134 ⁱ⁾ in sulfuric acid, ref. 135 ^{j)} in sulfuric acid, ref. 136 ^{k)} in acetic acid, ref. 137 ^{l)} in trifluoroacetic acid, UV spectrum: sulfuric acid, ref. 138 ^{m)} in acetonitrile, ref. 139 ⁿ⁾ in acetonitrile, ref. 114 ^{o)} in a glassy matrix, ref. 84


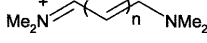
absorb at about 550 nm in nonpolar solvents. The calculated absorption wavelength of the color band is of the expected order of magnitude. The obviously low error is remarkable with regard to the formerly mentioned suspicion [22] that extensive charge separation may cause erratic DFT results. In contrast to the previously mentioned interfragmental charge-transfer (CT) transitions, intramolecular CT transitions of conjugated systems are obviously well reproduced by TDDFT.

Lüttke's parent thioindigo chromophore [76] is exemplified by **54** [77]. A long-wavelength $\pi \rightarrow \pi^*$ transition is calculated which brings about the orange-red color of **53**. In agreement with experiment, thioindigo (**55**) is

calculated to be more bathochromic than **53** [77]. The spectral characteristics of the UV/vis spectrum of **54** is well reproduced both by TDDFT and by PPP calculations [78]. The color band is caused by an intense lowest-energy transition of the symmetry $B_u \leftarrow A_g$ calculated at 508 nm (experiment 546 nm) (Table 2). It is not well understood why ZINDO/S does not reproduce the color of the indigoid compounds **54** and **55**, placing the first intense transition in the NUV. The TDDFT results agree very well with the long-wavelength absorption band of the green-colored monothioanthraquinone (**56**) (Table 2). The first weak band is due to the $n \rightarrow \pi^*$ transition of the thiocarbonyl group and the intense shorter-

Table 3. Calculated and experimental absorption wavelengths of parent cyanine dyes

						
	TDDFT	ZINDO/S	Exp. ^{a)}	TDDFT	ZINDO/S	Exp. ^{b)}
n = 0	309 (0.21)	293 (0.37)	333			
n = 1	367 (0.88)	367 (0.89)	414	229 (0.38)	268 (0.76)	268 (4.43)
n = 2	398 (1.36)	436 (1.47)		298 (0.89)	362 (1.26)	363 (4.75)
n = 3	446 (1.89)	506 (2.01)		351 (1.42)	433 (1.74)	455 (4.99)
n = 4	495 (2.40)	579 (2.74)		404 (1.90)	503 (2.25)	548 (4.80)
n = 5	–	–		455 (2.36)	572 (2.49)	

						
	TDDFT	ZINDO/S	Exp. ^{c)}	TDDFT ^{e,f)}	ZINDO/S ^{e)}	Exp. ^{d)}
n = 0	252 (0.32)	260 (0.33)	299	163 (0.38)	195 (0.44)	224 (4.16)
n = 1	305 (0.78)	321 (0.80)		235 (0.74)	289 (0.90)	314 (4.81)
n = 2	381 (1.13)	398 (1.35)		301 (1.16)	363 (1.37)	416 (5.08)
n = 3	411 (1.73)	419 (1.82)		360 (1.59)	432 (1.84)	519 (5.32)
n = 4	460 (2.19)	475 (2.22)		415 (2.03)	499 (2.62)	625 (5.47)
n = 5	–	–		467 (2.48)	565 (2.62)	848 (5.44)

^{a)} in alkali, ref. 140

^{b)} in dimethylformamide, ref. 141

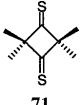
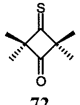
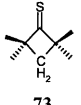
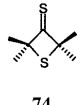
^{c)} in sulfuric acid, ref. 140

^{d)} in methylene chloride, ref. 141

^{e)} CH₃ replaced by H in TD-DFT and ZINDO/S calculations

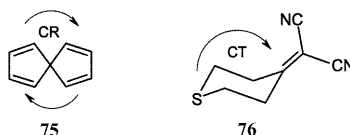
^{f)} PPP calculations [79] λ_{\max} in nm: 211 (n = 0) 317 (n = 1) 408 (n = 2) 497 (n = 3) 585 (n = 4) 671 (n = 5); ZINDO/S (this study) 195 (n = 0) 289 (n = 1) 363 (n = 2) 432 (n = 3) 500 (n = 4) 564 (n = 5)

Table 4. Calculated and experimental absorption wavelengths of 2,2,4,4-tetramethyl-cyclobutane-1,3-dithione and related monothiones in the near ultraviolet and visible region. Oscillator strengths f (calc.) and $\lg\epsilon$ values (exp.) in parenthesis^{a,b)}

					
		71	72	73	74
TD-DFT					
$n \rightarrow \pi^*$	EX_{CS}^+ (A_u)	539 (0.0)	$LE_{S \rightarrow CS}$ 523	$LE_{S \rightarrow CS}$ 495	$LE_{S \rightarrow CS}$ 485
$n \rightarrow \pi^*$	EX_{CS}^- (B_{3g})	493 (0.0)	$CT_{O \rightarrow CS}$ 361		
$n \rightarrow \pi^*$	CR_{CS}^+ (B_{3g})	399 (0.0)	$CT_{S \rightarrow CO}$ 306		$CT_{S \rightarrow CS}$ 407
$n \rightarrow \pi^*$	CR_{CS}^- (A_u)	378 (0.0)	$LE_{O \rightarrow CO}$ 274		
$\pi \rightarrow \pi^*$	EX_{CS}^+ (B_{3u})	219 (0.50)	LE_{CS} 227	LE_{CS} 227	
ZINDO/S					
$n \rightarrow \pi^*$	EX_{CS}^+ (B_{3g})	513 (0.0)	LE_{CS} 509	LE_{CS} 491	LE_{CS} 519
$n \rightarrow \pi^*$	EX_{CS}^- (A_u)	505 (0.0)	$LE_{O \rightarrow CS}$ 407		
$n \rightarrow \pi^*$	CR_{CS}^+ (A_u)	240 (0.0)			
$n \rightarrow \pi^*$	CR_{CS}^- (B_{3g})	238 (0.0)			
$\pi \rightarrow \pi^*$	EX_{CS}^+ (B_{3u})	228 (0.67)	LE_{CS} 219	LE_{CS} 222	$CT_{S \rightarrow CS}$ 236
Exp.^{c)}					
A		500 (1.35)	520 (0.98)	500 (1.08)	–
B		298 (2.61)	328 (2.07)	233 (3.87)	–
			272sh (2.5)		
C		227 (4.33)	228 (3.94)	218 (3.72)	–

^{a)} EX = exciton-type, CR = charge-resonance-type, CT = charge-transfer-type transition

^{b)} Two compounds for comparison calculated by TDDFT:



Spiro[4,4]nonatetraene (D_{2d} -symmetry) (**75**) is known to absorb at 268 nm weakly 212 nm strongly in hexane [111]. The degenerate EX and CR transitions are calculated at 317 ($f < 0.01$, $E \leftarrow A_1$) and 234 nm ($f = 0.07$, $E \leftarrow A_1$), resp.

4,4-Dinitrilovinylidenethiacyclohexane (C_s -symmetry) (**76**) displays an absorption band at 294 nm in cyclohexane ($\lg\epsilon$ 3.46) [112] to compare with the calculated TDDFT CT transition at 375 nm ($f < 0.01$, $A \leftarrow A$)

^{c)} Experimental absorption wavelengths of **70** and **71** [86] and **72** in [143] hexane

wavelength band is due to the $\pi \rightarrow \pi^*$ transition. In this case, TDDFT and ZINDO/S provide comparable results (Table 2).

The calculated wavelength of the first intense band may be markedly underestimated, however, for merocyanine and cyanine dyes (“polymethine dyes”). The longest-wavelength absorption of the meropolymethine-type dyes 1,2-dithiol-2,2-ylidene acetaldehyde (**57**), 4-(1,3-benzodithiol-2-ylidene)cyclohexadien-1-one (**58**) and the *syn*-pyramidalized 2-(thioxanthen-9-ylidene)indane-1,3-dione (**59**) are calculated at wavelengths too short (Table 2). The erratic blueshift of the calculated wavelengths of the color bands increases in passing from the tetrathiaporphyrine dication (**60**) to the bisthiénylmetinium cation (**61**) to the open-chain polymethine dye **62**. The error in the calculation of the red–blue colored **62** amounts to about 0.74 eV. This same type of error is found in the various vinylogous series of polymethine dyes (Table 3). These dyes display intense long-wavelength absorptions owing to long-axis polarized $\pi \rightarrow \pi^*$ transitions ($B_2 \leftarrow A_1$). Whereas the experimental absorption wavelengths of the intense first band of these dyes increase by about 100 nm with the consecutive ex-

tension of the chromophoric system by one double bond (“vinylene shift”) [78–81] the calculated shift is much too low. This is demonstrated by calculation of the thioxonol anions (**63**) and thiacyanine cations (**64**) reported in Table 3 and, for comparison, with the experimentally better known related oxonol (**65**) and cyanine dye (**66**) series. The calculated vinylene shift between the higher vinylogues in the last-mentioned series was half as large as found experimentally (about 100 nm). The same failure was also observed in the time-dependent local density in the DFTB–TDLDA [27]. Polymethines are distinguished from other conjugated chain molecules by a local CT at the methine groups in passing from the ground state to the lowest-energy π , π^* excited state [78–81]. It should be mentioned that the vinylene shift is also underestimated by single-configuration-based CIS calculations at the ab initio level, while the semiempirical PPP and ZINDO/S calculations provide results less in error (footnote to Table 4). The absorption wavelengths, however, are also underestimated at larger chain lengths at these semiempirical levels [79]. Nishimito [82] discussed the weakness of the PPP method in terms of Parr’s softness concept, proposing

a reduction of the two-center two-electron repulsion integrals in the PPP approximation. Surprisingly, most approximate MO approaches, such as Hückel's MO models [82] and Kuhn's MO model of the "free electron" [83], treat the vinylene shift more correctly.

Although successful attempts are known to calculate organic radicals by TDDFT [17], calculations of spectral data based on the spin-unrestricted Kohn–Sham approach have to be considered with caution. Unfortunately, there is a lack of knowledge regarding experimental data of sulfur-organic radicals. Theoretical and experimental spectral data of **67–69** are listed in Table 2. Without doubt, the deviation between theory and experiment is generally larger than for nonradical compounds. The radicals mentioned in Table 2 are conjugated compounds derived from Hünig's polymethine violenes [80]. The longest-wavelength absorption of the Wurster-type radicals **67**, **68** und **69** were satisfactorily predicted in the visible or NUV regions. The recently extensively studied 2,2'-bisthiophene cation radical (**70**) [84] affords another example. The planar compound (C_{2h} symmetry) absorbs weakly at 590 nm and strongly at 425 nm in a low-temperature glassy matrix. These absorption bands were assigned by multiconfiguration linear response calculations with absorptions calculated at 606 and 447 nm [84]. The TDDFT data were less accurate (594 and 374 nm, Table 2).

Finally, 2,2,4,4-tetramethyl-1,3-cyclobutanedithione (**71**) is considered as an example of a simple bichromophoric system. The compound contains two thiocarbonyl groups which exhibit through-bond interaction [85–87]. The structure of **71** is supported by X-ray diffraction analysis [88]. According to photoelectron spectroscopy the splitting of the first ionization energies due to the interaction of the lone pair orbitals at the sulfur atoms amounts to 0.5 eV [87]. The energies of the lowest-energy Kohn–Sham orbitals differ by the same order of magnitude (about 0.4 eV). TDDFT predicts three regions of light absorption: two absorption bands at about 400 and 500 nm due to four $n \rightarrow \pi^*$ type transitions and one intense absorption band in the near UV due to the intense $\pi \rightarrow \pi^*$ type transition. The first two absorptions originate in four forbidden transitions of $A_u \leftarrow A_g$ and $B_{3g} \leftarrow A_g$ symmetry, followed by an intense transition of $B_{3u} \leftarrow A_g$ symmetry. The experimental data given in Table 4 reflect the calculated result in general, except for the second absorption band, B. The electron transition of this absorption band was calculated at about 400 nm rather than the 300 nm as found by experiment (0.99 eV in error). According to the composite-molecule model [1] these transitions are of the interfragmental CT type, with one-electron excitations from the lone pairs on the sulfur atoms of each thiocarbonyl group to the π^* LUMOs of the other thiocarbonyl group (also called charge-resonance transition, CR). The intense absorption at 230 nm (band C) and the weak absorption (A) at 500 nm are well reproduced. The latter absorption is due to the local $n \rightarrow \pi^*$ transitions of the thiocarbonyl group that are combined to exciton-type (EX) transitions. The position of the EX-type band of **70** is at nearly the same wavelengths as in **72** and **73** (Table 4).

It is not clear whether the error in calculating CR-type bands is more general. A TDDFT test calculation of the spiro[4,4]nonatetraene (**75**) with two weakly in-

teracting $\pi\pi^*$ chromophores [87] led to a deviation twice as large than the mean average deviation (0.5 eV, cf. data in the footnote to Table 4).

Whereas the lowest-energy transition of **72** at about 500 nm is a local $LE_{S \rightarrow CS}$ type ($n \rightarrow \pi^*$) transition as found for **73**, the next higher-energy transitions are interfragmental $CT_{O \rightarrow CS}$ and $CT_{S \rightarrow CO}$ transitions. The calculated CT transitions and the local $n \rightarrow \pi^*$ transition at the C=O group ($LE_{O \rightarrow CO}$) of **72** obviously cause the experimentally found B band. The calculation seems to be not much in error. A weak CT-type band at about 300 nm is also calculated and found experimentally [89] when the carbonyl group of **72** is replaced by dicyanovinylene group ($=CCN)_2$). In the experimentally unknown **74** the p_π orbital of the ring sulfur should be the electron donor and the thiocarbonyl group the electron acceptor. A long-wavelength $CT_{S \rightarrow CS}$ transition is expected at about 400 nm. ZINDO/S calculations results in a shorter-wavelength transition in the NUV. To check the possible error in the calculation of interfragmental CT transition energies of weakly interacting structures, the spectroscopically well-studied 4,4'-dicyanovinylidene-thiacyclohexane (**76**) was calculated. As verified experimentally [90], the relatively weak absorption of **76** at 294 nm is of the CT type. The TDDFT calculation, however, again provides an absorption at nearly 100 nm longer wavelengths (0.91 eV in error) (cf footnote to Table 4). The next-highest transition is overwhelmingly localized at the $C=(CN)_2$ group and is correctly calculated at 238 nm (experiment 230 nm). Thus, as found with the erratic interpeptide CT transition [22], the CT transition absorption wavelengths of composite donor–acceptor systems are in error. In the case of the spiro compound **75** the error was, however, less. Although structures such as **76** are of great interest in photo-physical studies, such as in electron-transfer processes, they play a minor role as chromophoric systems. While caution must be exercised in the calculation of CT transitions in bichromophoric structures, intramolecular CT transitions in delocalized π systems are obviously well reproduced by TDDFT calculations.

4 Conclusions

Without introducing any particular parameters, absorption characteristics of a test series of sulfur-organic compounds of very different structures are well reproduced by TDDFT calculations. The average absolute deviation of the calculated spectral data from the experimental data for transitions that were compared amounts to 0.21 eV. A more detailed analysis has shown that the deviation is distinctly different for $n \rightarrow \pi^*$ (0.09 eV) and for $\pi \rightarrow \pi^*$ transitions (0.24 eV). The low-energy $n \rightarrow \sigma^*$ and $\sigma \rightarrow \pi^*$ type transitions of disulfides are well calculated by TDDFT but not at the semiempirical ZINDO/S level of theory. As expected ZINDO/S works reasonably well for $n \rightarrow \pi^*$ and $\pi \rightarrow \pi^*$ transitions, with an errors of 0.09 and 0.40 eV, respectively. The application of the PPP method is naturally restricted to $\pi \rightarrow \pi^*$ transitions of planar compounds. With an absolute mean deviation of 0.20 eV the performance of PPP is

comparable with that of TDDFT and is much better than that of ZINDO/S for the same series of compounds. ZINDO/S fails for disulfidic structures. As long as only $n \rightarrow \pi^*$ and $\pi \rightarrow \pi^*$ are of interest, the semiempirical methods remain attractive because of the low computational time. However, TDDFT opens more general access to the various electronic transitions. The good performance of TDDFT was demonstrated with different types of electronic transitions arising from the all-valence electron system. Some additional data and applications of TDDFT in sulfur-organic chemistry are published elsewhere [91].

Limitations of TDDFT were encountered with CT-type transitions if the transition occurs between donor and acceptor fragments separated on molecular fragments in a single molecule (composite molecules with through-space interaction). In this case the absorption wavelengths are overestimated (deviations up to 1 eV in energy). The absorptions of long-chain cyanine dyes are calculated at wavelengths much too short. The so-called "vinylene shift" of polymethine dyes is not reproduced.

Compared with other first-principles methods the application of TDDFT proved to be particularly attractive and broadly applicable. The method is a good compromise between accuracy and computational demand. Linear scaling of TDDFT will help to save computer time in future.

Acknowledgements. This study has benefited from stimulating discussions with G. Seifert (Paderborn). I am indebted to H.-U. Wagner (Munich) for some PPP calculations with the recently developed wPSIN3F program and E. Lewars (Peterborough, Canada) for the critical perusal of the manuscript. I would like to thank M. Mann (Dresden) for computational assistance. The Deutsche Forschungsgemeinschaft and the Fonds der Chemischen Industrie supported this work.

Note added in proof

Adamo et al. have shown that accurate excitation energy calculations of closed and open shell compounds absorbing in the near and far ultraviolet are obtained by combining the Perdew-Burke-Erzenrhof generalized gradient functional with a predetermined amount of the exact exchange (PBE0 model). Transition metal complexes were also calculated.

(a) Adamo C, Barone V (2000) *Theor Chem Acc* 105: 169; (b) Adamo C, Scuseria GE, Barone V (1999) *J Chem Phys* 111: 2889; (c) Adamo C, Barone V (1999) *Chem Phys Lett* 314: 152

The application of TDDFT for electronic transition calculations of polyenes with significant double excitation character has been discussed recently.

Hsu C-P, Hirata S, Head-Gordon M (2001) *J Phys Chem A* 105:451

The linear scaling technique was applied to DFT.

van Gisbergen SJA, Guerra CF, Baerends EJ (2000) *J Comput Chem* 21:1511

References

1. Suzuki H (1967) *Electronic absorption spectra and geometry of organic molecules*. Academic, New York
2. (a) Zerner MC (1991) In: Lipkowitz KB, Boyd DB (eds) *Reviews of computational chemistry*, vol 2. VCH, New York, pp 313 ff, and references therein; (b) Lauer G, Schulte K-W,

- Schweig A (1978) *J Am Chem Soc* 100: 4925; (c) Montero LA, Alfonso L, Alvarez JR, Perez E (1990) *Int J Quant Chem* 37: 465
3. (a) Pfister-Guillouzo G, Gonbeau D, Deschamps J (1972) *J Mol Struct* 14: 81; (b) Takata S, Ono, Y, Ueda Y (1985) *Chem Pharm Bull* 33: 3077; (c) Buemi G (1993) *Gazz Chim Ital* 123: 379
4. Ridley J, Zerner M (1973) *Theor Chim Acta* 32: 111
5. Herman ZS, Kirchner EF, Loew GH, Mueller-Westerhoff UT, Nazaal A, Zerner MC (1982) *Inorg Chem* 21: 46
6. (a) Ertl P, Leska J (1988) *J Mol Struct* 165: 1; (b) Clark T, Chandrasekhar J (1994) *Isr J Chem* 33: 435
7. Hase HL, Lauer G, Schulte K-W, Schweig A (1978) *Theor Chim Acta* 48: 47
8. Foresman JB, Head-Gordon M, Pople JA, Frisch MJ (1992) *J Phys Chem* 96: 135
9. (a) Stanton JF, Bartlett RJ (1993) *J Chem Phys* 98: 7029; (b) Christiansen O, Jorgensen P (1998) *J Am Chem Soc* 120: 3423; (c) Gwaltney SR, Bartlett RJ (1998) *J Chem Phys* 108: 6790; (d) Nooijen M (2000) *J Phys Chem A* 104: 4543
10. Werner H-J (1987) In: Lawley KP (ed) *Ab initio method in quantum chemistry*, part 2. Wiley, Chichester, pp 1 ff
11. (a) Roos BO (1987) In: Lawley KP (ed) *Ab initio method in quantum chemistry*, part 2. Wiley, Chichester, pp 399 ff (b); Roos BO (1999) *Acc Chem Res* 32: 137; (c) Merchán M, Serrano-Andrés L, Gonzales-Luque R, Roos BO, Rubio M (1999) *J Mol Struct (THEOCHEM)* 197–200: 201, and references therein
12. (a) Serrano-Andrés L, Merchán M, Fülcher M, Roos BO (1993) *Chem Phys Lett* 211: 125; (b) Rubio M, Merchán M, Orti E, Roos BO (1995) *J Chem Phys* 102: 3580; (c) Rubio M, Merchán M, Orti E, Roos BO (1996) *Chem Phys Lett* 248: 321
13. Koch W, Holthausen MC (2000) *A chemist's guide to density functional theory*. Wiley-VCH, Weinheim, pp 63 ff, 169 ff
14. Bauernschmitt R, Ahlrichs R (1996) *Chem Phys Lett* 256: 454
15. (a) Bauernschmitt R, Häser M, Treutler O, Ahlrichs R (1997) *Chem Phys Lett* 264: 573; (b) Wiberg KB, Stratmann RE, Frisch MJ (1998) *Chem Phys Lett* 297: 60
16. Stratmann RE, Scuseria GE, Frisch MJ (1998) *J Chem Phys* 109: 8218
17. Hirata S, Head-Gordon M (1999) *Chem Phys Lett* 302: 375
18. Casida ME, Jamorski C, Casida KC, Salahub DR, (1998) *J Chem Phys* 108: 4439
19. Heinze HH, Görling A, Rösch N (2000) *J Chem Phys* 113: 2088
20. Sundholm D (1999) *Chem Phys Lett* 302: 480
21. van Gisbergen SJA, Rosa A, Ricciardi G, Baerends EJ (1999) *J Chem Phys* 111: 2499
22. Tozer TJ, Amos RD, Handy NC, Roos BO, Serrano-Andrés L (1999) *Mol Phys* 97: 859
23. Hirata S, Head-Gordon M (1999) *Chem Phys Lett* 314: 291
24. Grimme S (1996) *Chem Phys Lett* 259: 128
25. Parusel ABJ, Wondimagegn T, Ghosh A (2000) *J Am Chem Soc* 122: 6371
26. Grimme S, Waletzke M (1999) *J Chem Phys* 111: 5644
27. Niehaus T, Suhai S, Della Sala F, Elstner H, Seifert G, Frauenheim T (2001) *Phys Rev B* 63: 85–108
28. Petiau M, Fabian J, Rosmus P (1999) *Phys Chem Chem Phys* 1: 5547
29. Fabian J, Mann M, Petiau M (2000) *J Mol Model* 6: 177
30. Frisch MJ, Trucks GW, Schlegel HB, Scuseria GE, Robb MA, Cheeseman JR, Zakrzewski VG, Montgomery JA Jr, Stratmann RE, Burant JC, Dapprich S, Millam JM, Daniels AD, Kudin KN, Strain MC, Farkas O, Tomasi J, Barone V, Cossi M, Cammi R, Mennucci B, Pomelli C, Adamo C, Clifford S, Ochterski J, Petersson GA, Ayala PY, Cui Q, Morokuma K, Malick DK, Rabuck AD, Raghavachari K, Foresman JB, Cioslowski J, Ortiz JV, Baboul AG, Stefanov BB, Liu G, Liashenko A, Piskorz P, Komaromi I, Gomperts R, Martin RL, Fox DJ, Keith T, Al-Laham MA, Peng CY, Nanayakkara A, Gonzalez C, Challacombe C, Gill PMW, Johnson W, Chen W, Wong MW, Andres JL, Head-

- Gordon M, Replogle ES, Pople JA (1998) Gaussian98, revision A.7. Gaussian, Pittsburgh, Pa
31. (a) Becke AD (1993) *J Chem Phys* 98: 1372; (b) Becke AD (1993) *J Chem Phys* 98: 5648; (c) Lee C, Yang W, Parr RG (1988) *Phys Rev B* 37: 785; (d) Hu C-H, Chong DP (1998) In: Schleyer PvR, Allinger NL, Clark T, Kollman PA, Schaeffer HF III, Gasteiger J (eds) *Encyclopedia of computational chemistry*, vol 1. Wiley, New York, pp 664 ff, and references therein
 32. (a) Hargittai I (1985) *The structure of volatile sulphur compounds*. Akadémiai Kiadó, Budapest; (b) Georgiou K, Kroto HW (1980) *J Mol Spectrosc* 83: 94; (c) Corkill MJ, Cox P, Ewart IC (1976) *J Chem Soc Chem Commun* 546
 33. Ma B, Lii J-H, Schaeffer HF III, Allinger NL (1996) *J Phys Chem* 100: 8763
 34. Wagner H-U, Fabian J (1997) wPSIN3, PPP Singlet-CI Program 97.11. Ludwigs-Maximilian Universität München, Technische Universität Dresden
 35. Fabian J, Tröger G (1971) *Teor Eksp Khim* 7: 170
 36. Fabian J, Mehlhorn A, Zahradnik R (1968) *J Phys Chem* 72: 3975
 37. Fabian J, Mehlhorn A, Tröger G (1967) *Theor Chim Acta* 9: 140
 38. (a) Fabian J (1972) *Z Phys Chem (Leipzig)* 250: 377; (b) Fabian J, Mehlhorn A (1967) *Tetrahedron Lett* 2049; (c) Fabian J, Hartmann H (1973) *Tetrahedron* 29: 2597; (d) Hartmann H, Fabian J (1969) *Ber Bunsenges Phys Chem* 73: 107
 39. Hartmann H, Fabian K, Fabian J (1968) *Theor Chim Acta* 12: 319
 40. (a) Kasha M (1950) *Discuss Faraday Soc* 9: 14; (b) Suzuki H (1967) *Electronic absorption spectra and geometry of organic molecules*. Academic, New York, p 537
 41. Schaftenaar G (2000) *Molden*, release 3.6. Nijmegen
 42. Schaumann E (1989) In: Patai S (ed) *The chemistry of double-bonded functional groups*. Wiley, Chichester, pp 1269–1367
 43. Rosengren K (1962) *Acta Chem Scand* 16: 1401
 44. Fabian J, Mayer R (1964) *Spectrochim Acta* (1964) 20: 299
 45. Judge RH, Drury-Lessard CR, Moule DC (1978) *Chem Phys Lett* 53: 82
 46. (a) Burton PG, Peyerimhoff SD, Buenker RJ (1982) *Chem Phys* 73: 83; (b) Buenker RJ, Peyerimhoff SD (1977) *Chem Phys* 22: 375
 47. Falk KJ, Steer RP (1968) *Can J Chem* 66: 575
 48. Lightner DA, Bouman TD, Donald Wijekoon WM, Hansen AE (1984) *J Am Chem Soc* 106: 934
 49. Serafimov O, Brühlmann U, Huber JR (1975) *Ber Bunsenges Phys Chem* 79: 202
 50. Fabian J, Laban G (1969) *Tetrahedron* 25: 1441
 51. Fabian J (1973) *Z Chem* 13: 26
 52. Pfister-Guillouzo G, Gonbeau D, Deschamps J (1972) *J Mol Struct* 14: 95
 53. (a) Robin MB (1974) *Higher excited states of polyatomic molecules*, vol 1. Academic, New York, p 287; (b) Thompson SD, Carroll DG, Watson F, O'Donnell M, McGlynn SP (1966) *J Chem Phys* 45: 1367; (c) Tokue I, Hiraya A, Shobatake K (1989) *Chem Phys* 130: 401
 54. Williams DR, Kontnik LT (1971) *J Chem Soc* 312
 55. Gleiter R, Schmidt E, Johnson P, Cowan DO (1973) *J Am Chem Soc* 95: 2860
 56. Demiralp E, Goddard WA III (1997) *J Phys Chem A* 101: 8128
 57. Hargittai I, Brunvoll J, Kolonits M, Khodorkovsky V (1994) *J Mol Struct* 317: 273
 58. Gleiter R, Schmidt E, Cowan DO, Ferraris JP (1973) *J Electron Spectrosc Relat Phenom* 2: 207
 59. Tajiri A, Hatano M, Yamamoto K, Murata I (1982) *Chem Phys* 91: 433
 60. Glass RS, Gruhn NE, Lichtenberger DL, Lorange E, Pollard JR, Birringer M, Block E, DeOrazio R, He C, Shan Z, Zhang X (2000) *J Am Chem Soc* 122: 5065
 61. Zweig A, Hoffmann AK (1965) *J Org Chem* 30: 3997
 62. Sandman DJ, Caesar GP, Nielsen P, Epstein AJ, Holmer HTJ (1978) *J Am Chem Soc* 100: 202
 63. Spanget-Larsen J, Erting C, Shim I (1994) *J Am Chem Soc* 116: 11433
 64. Takane S, Sakai S (1999) *J Mol Struct (THEOCHEM)* 488: 1
 65. Greenberg MM, Blackstock SC, Stone KJ, Berson JA (1989) *J Am Chem Soc* 111: 3671
 66. Fabian J, Hess BA Jr (1997) *J Org Chem* 62: 1766
 67. Fabian J, Senning A (1998) *Sulfur Rep* 21: 1
 68. Fabian J, Wolff T (1996) *J Photochem Photobiol B* 96: 1
 69. Młostoń G, Romański J, Reisenauer HP, Maier G (2001) *Angew Chem* 113: 401
 70. Ollis WD, Ramsden CA (1976) *Adv Heterocycl Chem* 19: 1
 71. Gotthardt H, Weissshuhn MC, Christl B (1976) *Chem Ber* 109: 740
 72. Schönberg A, Frese E (1970) *Chem Ber* 103: 3885
 73. Reichhardt C (1994) *Chem Rev* 94: 2319, and references given therein
 74. Fabian J, Rosquete GA, Montero-Cabrera LA (1999) *J Mol Struct (THEOCHEM)* 469: 163
 75. Gonzales D, Neilands O, Rezende MC (1999) *J Chem Soc Perkin Trans* 713
 76. Klessinger M (1966) *Tetrahedron* 22: 3355
 77. Hermann H, Lüttke W (1968) *Chem Ber* 101: 1715
 78. Fabian J, Hartmann H (1980) *Light absorption of organic colorants*. Springer, Berlin Heidelberg New York
 79. Fabian J, Zahradnik R (1977) *Wiss Z Techn Univ Dresden* 26: 315
 80. Tyutyulkov N, Fabian J, Mehlhorn A, Tadjer A (1991) *Polymethine dyes*. St Kliment Ohridski University Press, Sofia
 81. Fabian J, Hartmann H (1975) *J Mol Struct* 27: 67, and references therein
 82. Nishimoto K (1993) *Bull Chem Soc Jpn* 66: 1877
 83. (a) Kuhn H (1958) *Fortschr Chem Org Naturst* 16: 169; (b) Kuhn H (1959) *Fortschr Chem Org Naturst* 17: 404
 84. Keszthely T, Grage MM-L, Offersgaard JF, Wilbrandt R, Svendsen C, Mortensen OS, Pedersen JK, Jensen HJA (2000) *J Phys Chem A* 104: 2808
 85. (a) Ballard RE; Park CH (1970) *Spectrochim Acta A* 26: 43; (b) Trabjerg I, Vala M, Baiardo J (1983) *Mol Phys* 50: 193
 86. Elam EU, Davies HE (1967) *J Org Chem* 32: 1562
 87. Gleiter R, Spanget-Larsen J (1979) *Top Curr Chem* 86: 139
 88. Shirrell CD, Williams DE (1973) *Acta Crystallogr B* 29: 1648
 89. Rao B, Chandrasekhar J, Ramamurthy V (1988) *J Org Chem* 53: 745
 90. Pasma P, Verhoeven JW, Boer TJ (1977) *Tetrahedron Lett* 207
 91. Petiau M, Fabian J (2001) *J Mol Struct (THEOCHEM)* 538: 253
 92. Judge RH, Moule DC, Bruno AE, Steer RP (1983) *Chem Phys Lett* 102: 385
 93. Giles HG, Marty RA, De Mayo P (1976) *Can J Chem* 54: 537
 94. De Mayo P, Weedon AC, Wong GSK (1979) *J Org Chem* 44: 1977
 95. Metzner P, Vialle J (1972) *Bull Soc Chim Fr* 3138
 96. Rao VP, Ramamurthy V (1988) *J Org Chem* 53: 327
 97. Gebauer H (1960) *Doctoral dissertation*. Technische Universität München
 98. Machiguchi T, Otani H, Ishii Y, Hasegawa T (1987) *Tetrahedron Lett* 28: 203
 99. (a) Davis RE (1958) *J Org Chem* 23: 216, (b) Davis RE (1958) *J Org Chem* 23: 1380; (c) Challenger F, Mason EA, Holdsworth EC, Emmott R (1953) *J Chem Soc* 292
 100. Price CC, Morita H (1953) *J Am Chem Soc* 75: 4747
 101. Dittmer DC, Takahashi K, Davis FA (1967) *Tetrahedron Lett* 4061
 102. Strating J, Keijer JH, Molenaar E, Brandsma L (1962) *Angew Chem* 76: 465
 103. (a) Nyulási Z, Veszprémi T (1986) *Chem Scr* 26: 629 (b) Nyulási Z, Veszprémi T (1988) *Chem Scr* 28: 331; (c) Di

- Lonardi G, Galloni G, Trombetti A, Zauli C (1972) *J Chem Soc Faraday Trans II* 68: 2009
104. Litvinov IP, Goldfarb YL (1976) *Adv Heterocycl Chem* 19: 123, and references therein
105. Schweig A, Diehl F, Kesper K, Meyer H (1986) *J Mol Struct* 198: 307
106. Angeloni AS, Tramontini M (1963) *Ann Chim (Rome)* 53: 1665
107. Mayer R, Kleinert H, Richter S, Gewald K (1962) *Angew Chem* 74: 118
108. Abu-Eittah RH, Al-Sugeir FA (1985) *Bull Chem Soc Jpn* 58: 2126
109. Mayer R, Franke J (1965) *J Prakt Chem* 30: 262
110. Anderson AG Jr, Harrison WF, Anderson RG (1963) *J Am Chem Soc* 85: 3448
111. O'Brien S, Smith DCC (1963) *J Chem Soc* 2907
112. Schlessinger RM, Ponticello GS (1967) *J Am Chem Soc* 89: 3641
113. Coffen DL, Chambers JQ, Williams DR, Garrett PE, Canfield ND (1971) *J Am Chem Soc* 93: 2258
114. Hünig S, Garner BJ, Ruider G, Schenk W (1973) *Liebigs Ann Chem* 1036
115. Yamamoto K, Yamazaki S, Kohashi Y, Murata I, Kai Y, Kanehisa N, Miki K, Kasai N (1982) *Tetrahedron Lett* 23: 3195
116. Parham WE, Wynberg H, Ramp FL (1953) *J Am Chem Soc* 75: 2065
117. Block E, Birringer M, DeOrazio R, Fabian J, Glass RS, Guao C, He C, Lorance ED, Qian Q, Schroeder TB, Shan Z, Thiruvazhi M, Wilson GS, Zhang X (2000) *J Am Chem Soc* 122: 5052
118. Brandt GRA, Emelús HJ, Haszeldine RN (1952) *J Chem Soc* 2549
119. Nelander B (1971) *Acta Chem Scand* 25: 1510
120. Dingwill JG, McKenzie S, Reid DH (1968) *J Chem Soc C* 2543
121. Leaver D, Robertson WAH, McKinnon DM (1962) *J Chem Soc* 5104
122. Degani I, Fochi R, Vincenzi C (1964) *Gazz Chim Ital* 94: 203
123. Lüttringhaus A, Engelhard N (1960) *Chem Ber* 93: 1525
124. Föhlich B, Haug E (1971) *Chem Ber* 104: 2324
125. Mlostoń G, Romański J, Schmidt C, Reisenauer HP, Maier G (1994) *Chem Ber* 127: 2527
126. Cava MP, Husbands GEM (1969) *J Am Chem Soc* 91: 3952
127. Hoffman JM Jr, Schlessinger RH (1969) *J Am Chem Soc* 91: 3953
128. Potts KT, McKeough D (1974) *J Am Chem Soc* 96: 4268
129. Acheson RM, Harrison DR (1970) *J Chem Soc* 1764
130. Prochazka M (1965) *Collect Czech Chem Commun* 30: 1158
131. Raasch MS (1979) *J Org Chem* 44: 632
132. Blanchard-Desce M, Ledoux I, Lehn J-M, Malthte J, Zyss J (1988) *J Chem Soc Chem Commun* 737
133. Gompper R, Wagner H-U (1968) *Tetrahedron Lett* 165
134. Stezowski JJ, Biedermann PU, Hildenbrand T, Dorsch JA, Eckhardt CJ, Agranat I (1993) *J Chem Soc Chem Commun* 213
135. (a) Vogel E, Röhrig P, Sicken M, Knipp B, Herrmann A, Pohl HS, Schmickler H, Lex J (1989) *Angew Chem* 101: 1883; (b) Vogel E, Röhrig P, Sicken M, Knipp B, Herrmann A, Pohl HS, Schmickler H, Lex J (1989) *Angew. Chem Int Ed Engl* 28: 1651
136. Lavrushin VF, Tsukerman CV, Syrovotka IG (1961) *Zh Obshch Khim* 31: 1275
137. Wizinger R, Dürr D (1963) *Helv Chim Acta* 46: 2167
138. (a) Fava A, Sogo PB, Calvin M (1957) *J Am Chem Soc* 79: 1078, (b) Fava A, Sogo PB, Calvin M (1957) *J Chem Soc* 213
139. Kießlich G (1968) Doctoral thesis. Universität Würzburg
140. Fabian J, Hartmann H (1973) *Tetrahedron* 29: 2597
141. Malhotra SS, Whiting MC (1960) *J Chem Soc* 3812
142. Batich C, Heilbronner E, Rommel E, Semmelhack MF, Foos JS (1974) *J Am Chem Soc* 96: 7662
143. Krebs A, Rüter W, Ziegenhagen B, Hebold M, Hardtke I, Müller R, Schütz M, Wietzke M, Wilke M (1984) *Chem Ber* 117: 277